NASA/CR-2009-215769

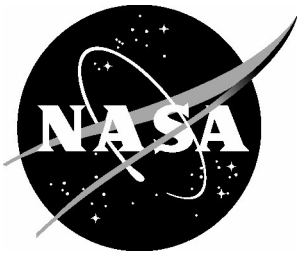

A Methodology for Determining Statistical Performance Compliance for Airborne Doppler Radar with Forward-Looking Turbulence Detection Capability

Roland L. Bowles and Bill K. Buck
AeroTech Research (U.S.A.), Inc., Newport News, Virginia

June 2009

The NASA STI Program Office . . . in Profile

Since its founding, NASA has been dedicated to the advancement of aeronautics and space science. The NASA Scientific and Technical Information (STI) Program Office plays a key part in helping NASA maintain this important role.

The NASA STI Program Office is operated by Langley Research Center, the lead center for NASA's scientific and technical information. The NASA STI Program Office provides access to the NASA STI Database, the largest collection of aeronautical and space science STI in the world. The Program Office is also NASA's institutional mechanism for disseminating the results of its research and development activities. These results are published by NASA in the NASA STI Report Series, which includes the following report types:

- TECHNICAL PUBLICATION. Reports of completed research or a major significant phase of research that present the results of NASA programs and include extensive data or theoretical analysis. Includes compilations of significant scientific and technical data and information deemed to be of continuing reference value. NASA counterpart of peer-reviewed formal professional papers, but having less stringent limitations on manuscript length and extent of graphic presentations.

- TECHNICAL MEMORANDUM. Scientific and technical findings that are preliminary or of specialized interest, e.g., quick release reports, working papers, and bibliographies that contain minimal annotation. Does not contain extensive analysis.

- CONTRACTOR REPORT. Scientific and technical findings by NASA-sponsored contractors and grantees.

- CONFERENCE PUBLICATION. Collected papers from scientific and technical conferences, symposia, seminars, or other meetings sponsored or co-sponsored by NASA.

- SPECIAL PUBLICATION. Scientific, technical, or historical information from NASA programs, projects, and missions, often concerned with subjects having substantial public interest.

- TECHNICAL TRANSLATION. English-language translations of foreign scientific and technical material pertinent to NASA's mission.

Specialized services that complement the STI Program Office's diverse offerings include creating custom thesauri, building customized databases, organizing and publishing research results ... even providing videos.

For more information about the NASA STI Program Office, see the following:

- Access the NASA STI Program Home Page at *http://www.sti.nasa.gov*

- E-mail your question via the Internet to *help@sti.nasa.gov*

- Fax your question to the NASA STI Help Desk at (443) 757-5803

- Phone the NASA STI Help Desk at (443) 757-5802

- Write to:
  NASA STI Help Desk
  NASA Center for AeroSpace Information
  7121 Standard Drive
  Hanover, MD 21076-1320

NASA/CR-2009-215769

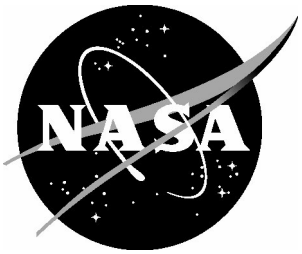

A Methodology for Determining Statistical Performance Compliance for Airborne Doppler Radar with Forward-Looking Turbulence Detection Capability

Roland L. Bowles and Bill K. Buck
AeroTech Research (U.S.A.), Inc., Newport News, Virginia

National Aeronautics and
Space Administration

Langley Research Center
Hampton, Virginia 23681-2199

Prepared for Langley Research Center
under Contract NNL06AA03B

June 2009

Acknowledgements

The authors would like to thank Jim Watson of NASA Langley Research Center for his guidance and leadership as the technical monitor in this effort. The authors would also like to acknowledge the members of the Federal Aviation Administration's Airborne Turbulence Detection Systems (ATDS) Industry Working Group for their support and participation in the development of the turbulence detection criteria. Finally, the authors would like to thank Dr. Paul Robinson and Steve Velotas of AeroTech Research for their efforts in the preparation and review of this document.

Available from:

NASA Center for AeroSpace Information
7121 Standard Drive
Hanover, MD 21076-1320
(443) 757-5802

Abstract

The objective of the research developed and presented in this document was to statistically assess turbulence hazard detection performance employing airborne pulse Doppler radar systems. The FAA certification methodology for forward–looking airborne turbulence radars will require estimating the probabilities of missed and false hazard indications under operational conditions. Analytical approaches must be used due to the near impossibility of obtaining sufficient statistics experimentally. This report describes an end-to-end analytical technique for estimating these probabilities for Enhanced Turbulence (E-Turb) Radar systems under noise-limited conditions, for a variety of aircraft types, as defined in FAA TSO-C134. This technique provides for one means, but not the only means, by which an applicant can demonstrate compliance to the FAA directed ATDS Working Group performance requirements. Turbulence hazard algorithms were developed that derived predictive estimates of aircraft hazards from basic radar observables. These algorithms were designed to prevent false turbulence indications while accurately predicting areas of elevated turbulence risks to aircraft, passengers, and crew; and were successfully flight tested on a NASA B757-200 and a Delta Air Lines' B737-800. Application of this defined methodology for calculating the probability of missed and false hazard indications taking into account the effect of the various algorithms used, is demonstrated for representative transport aircraft and radar performance characteristics.

Subject Terms

Aviation Safety, Turbulence, Turbulence Detection, Turbulence Encounters, Turbulence Reporting, Doppler Radar, Enhanced Airborne Weather Radar, Enhanced Turbulence (E-Turb), Airborne Remote Sensing, Detection Probability, Turbulence Hazard Metric, Weather, Safety, TSO-C134.

Table of Contents

1. Introduction and Background 1
2. Aircraft Centric Turbulence Hazard Metric Definition 3
3. Hazard Prediction Algorithm Design 4
4. Probability Calculations 6
   - 4.1 Formulation of Governing Equations 7
   - 4.2 Verification of Equation (5) and Equation (6) 8
     - 4.2.1 Conditions Defined for Monte-Carlo Simulation 8
     - 4.2.2 Radar y-Component of Hazard Algorithm 9
     - 4.2.3 Monte-Carlo Simulation Results 9
     - 4.2.4 Aircraft Weight "Strapped" Condition 11
5. Calculation of Nuisance and Missed Detection Probabilities 12
6. Technical Approach for Hazard Table Generation and "One-Size-Fits-All" Model for Class A Aircraft Systems 14
7. Conversion Factor PDFs for Class B and C Aircraft Systems 17
8. Radar Spectrum Width PDFs Based on Published Data 25
9. Application of Defined Methodology with Results for Class A Aircraft Systems 26
10. Summary and Conclusions 30
11. References 31

Appendix I: Calculation of Pulse Volume Compensation Factor

Appendix II: Inclusion of Radar Pulse Volume Compensation Factor in the Governing Probability Equations

List of Figures

Figure 1: Timeline of NASA Sponsored E-Turb Radar Research and Development 2

Figure 2: Correlation between Peak Load and Peak $\sigma_{\Delta n}$ (5 sec. window) 4

Figure 3: E-Turb Radar System Concept 6

Figure 4: PDF Comparison for 20,000 Flight Operations 10

Figure 5: CDF Comparison for 20,000 Flight Operations 11

Figure 6: Calculation of Nuisance and Missed Detection Probabilities Based on Hypothesis Testing 13

Figure 7: Technical Approach for Hazard Table Generation and "One-Size-Fits-All" Model for Class A Aircraft Systems 14

Figure 8: Class A Probability Density Functions for "One-Size-Fits-All" Algorithm Applicable for Aircraft Wing Loading between 80 and 135 lbs/ft^2 16

Figure 9: Technical Approach for Generating PDFs for Class B and C Aircraft Systems 18

Figure 10: Comparison of Scaled and OEM Data for a Class B Aircraft at 5,000 ft; 15,000 ft; 25,000 ft; and 35,000 ft 20

Figure 11: Comparison of Scaled and OEM Data for a Class B Aircraft at 10,000 ft; 20,000 ft; 30,000 ft; and 40,000 ft 21

Figure 12: Comparison of Scaled and OEM Data for a Class C Aircraft at 10,000 ft 21

Figure 13: Comparison of Scaled and OEM Data for a Class C Aircraft at 20,000 ft 22

Figure 14: Comparison of Scaled and OEM Data for a Class C Aircraft at 35,000 ft 22

Figure 15: Class B Probability Density Functions for "One-Size-Fits-All" Algorithm Applicable for Aircraft Wing Loading between 60 and 100 lbs/ft^2 23

Figure 16: Class C Probability Density Functions for "One-Size-Fits-All" Algorithm Applicable for Aircraft Wing Loading between 30 and 70 lbs/ft^2 24

Figure 17: Standard Deviation of Autocovariance (Pulse Pair) Estimator vs. Mean Spectral Width 26

Figure 18: Comparison of "One-Size-Fits-All" Performance and A320-200 with Weight Strapped Results for Extreme Operating Weights at Indicated Flight Conditions (5,000 ft) 28

Figure 19: Comparison of "One-Size-Fits-All" Performance and B777-200 with Weight Strapped Results for Extreme Operating Weights at Indicated Flight Conditions (5,000 ft) 29

Figure 20: Comparison of "One-Size-Fits-All" Performance and A320-200 with Weight Strapped Results for Extreme Operating Weights at Indicated Flight Conditions (35,000 ft) 29

Figure 21: Comparison of "One-Size-Fits-All" Performance and B777-200 with Weight Strapped Results for Extreme Operating Weights at Indicated Flight Conditions (35,000 ft) 30

List of Tables

Table 1: Comparison of z Statistics 10

Table 2: Example Format and Data for a Hazard Table for a Commercial Transport Aircraft (Class A) 16

Table 3: Class A Probability Density Functions for "One-Size-Fits-All" Algorithm Applicable for Aircraft Wing Loading between 80 and 135 lbs/ft^2 17

Table 4: Data Collected for Class B and C Aircraft Systems 18

Table 5: Class B Probability Density Functions for "One-Size-Fits-All" Algorithm Applicable for Aircraft Wing Loading between 60 and 100 lbs/ft^2 23

Table 6: Class C Probability Density Functions for "One-Size-Fits-All" Algorithm Applicable for Aircraft Wing Loading between 30 and 70 lbs/ft^2 24

Table 7: Weight Strapped x^0 Values 27

Table 8: Data Required for Calculating Must Indicate and Must Not Indicate Probabilities for the "One-Size-Fits-All" Model 27

Nomenclature

Acronym	Description
AIM	Aeronautical Information Manual
ARIES	Airborne Research Integrated Experiments System
ATDS	Airborne Turbulence Detection Systems
ATR	AeroTech Research (U.S.A.), Inc.
AvSSP	Aviation Safety and Security Program
CDF	Cumulative Distribution Function
DAL	Delta Air Lines
E-Turb	Enhanced Turbulence
FAA	Federal Aviation Administration
FFT	Fast Fourier Transform
FOQA	Flight Operations and Quality Assurance
ICAO	International Civil Aviation Organization
ISE	In-Service Evaluation
LIDAR	Light Detection And Ranging
MOPS	Minimum Operational Performance Standards
NASA	National Aeronautics and Space Administration
NTSB	National Transportation Safety Board
OEM	Original Equipment Manufacturer
PDF	Probability Density Function
RADAR	Radio Detection and Ranging
RMS	Root Mean Square
SNR	Signal-to-Noise Ratio
TAPS	Turbulence Auto-PIREP System
TPAWS	Turbulence Prediction and Warning Systems
TSO	Technical Standard Order
UAL	United Airlines
WxAP	Weather Accident Prevention

1. Introduction and Background

Turbulence has been identified as a significant operational aviation safety hazard during all phases of flight. Since 1998, the National Aeronautics and Space Administration (NASA) has conducted and funded research in the areas of turbulence detection and avoidance. Subsequently**,** NASA contracted AeroTech Research to conduct research and develop turbulence detection and avoidance systems in support of NASA's Aviation Safety and Security Program's (AvSSP) overall goal to "develop and demonstrate technologies that contribute to a reduction in aviation accident and fatality rates." From 1998 to 2003, AeroTech Research (and other NASA partners) developed the concepts and initial algorithms of various safety-related technologies under the NASA Turbulence Prediction and Warning Systems (TPAWS) element of the Weather Accident Prevention (WxAP) Project within AvSSP. The WxAP Program's three objectives to support the goal of the AvSSP were:

1. Develop technologies and methods that will provide pilots with sufficiently accurate, timely, and intuitive information during the en-route phase of flight, which, if implemented, will enable a 25-50% reduction in aircraft accidents attributable to lack of weather situational awareness.
2. Develop communications technologies that will provide a 3- to 5-fold increase in datalink system capacity, throughput, and connectivity for disseminating strategic weather information between the flight deck and the ground, which, if implemented along with other supporting technologies, will enable a 25-50% reduction in aircraft accidents attributable to lack of weather situational awareness.
3. Develop turbulence prediction technologies, hazard metric methods, and mitigation procedures to enable a 25-50% reduction in turbulence-related injuries.

Under the TPAWS element, the Enhanced Turbulence (E-Turb) Airborne Radar came to the forefront as a technology that was realizable and a significant contributor to meeting the TPAWS goal to "provide airborne centric technology for detection and cockpit display of hazardous turbulence" that when developed would "enable about a 50% reduction in injuries attributable to the lack of turbulence situational awareness." This technology was further developed and evaluated both in simulations and flight experiments onboard NASA's B757-200 ARIES Research Aircraft. The NASA flight experiments proved that the E-Turb Radar technology performed as designed and would provide the basis for much improved turbulence detection and awareness.

Engineering issues with the NASA B757 aircraft in late 2003 caused the cancellation of the TPAWS flight experiments for the E-Turb Radar technology. Realizing the importance of the research and needing a way to properly evaluate the technology, NASA and AeroTech Research sought collaboration within the aviation industry.

In August of 2003, a two-month feasibility study was initiated by NASA to develop the content and structure of a potential In-Service Evaluation (ISE) of the E-Turb Radar technology. The results of that study established a two-year ISE of the technology with the participation of Delta Air Lines (DAL) and Rockwell Collins. Reference [1] provides an overview and summary of the efforts, analyses, and results of the ISE initiatives. The specific objectives of the E-Turb Radar ISE were to implement and integrate E-Turb Radar algorithms within an airborne radar, install the radar onboard a commercial transport aircraft, and to evaluate the performance and effectiveness of the enhanced radar system in actual transport aviation operational environments over a reasonable timeframe. During the two year ISE, the E-Turb Radar algorithms were implemented into a WXR-2100 Multiscan^{TM} radar, which was installed into a B737-800 aircraft and flown over 3000 flight hours in operational service. The E-Turb Radar 1) performed as per design and intended function – provided improved, objective turbulence hazard detection and awareness relevant to the specific aircraft and its flight conditions; 2) received positive feedback from the flight crews; and 3) based on collected data and convincing evidence, was used by crews to avoid turbulence. The collected data also indicated strong correlation between E-Turb Radar

predicted loads and experienced loads when avoidance was not possible. Currently (June 2009), the ISE E-Turb Radar is still flying in operational service on the Delta B737-800.

The success of the E-Turb Radar ISE led NASA to direct AeroTech Research to investigate additional enhancements to the E-Turb Radar, an E-Turb capability with small radar antennas, a "one-size-fits-all" option for retrofitting E-Turb onto already installed radars, and an E-Turb Radar capability for regional jets and business jets (low wing loading aircraft). The results of this follow-on research indicated the feasibility of the application of E-Turb technology to a broad range of aircraft and radars. Figure 1 illustrates a timeline of the NASA-sponsored E-Turb Radar development activities.

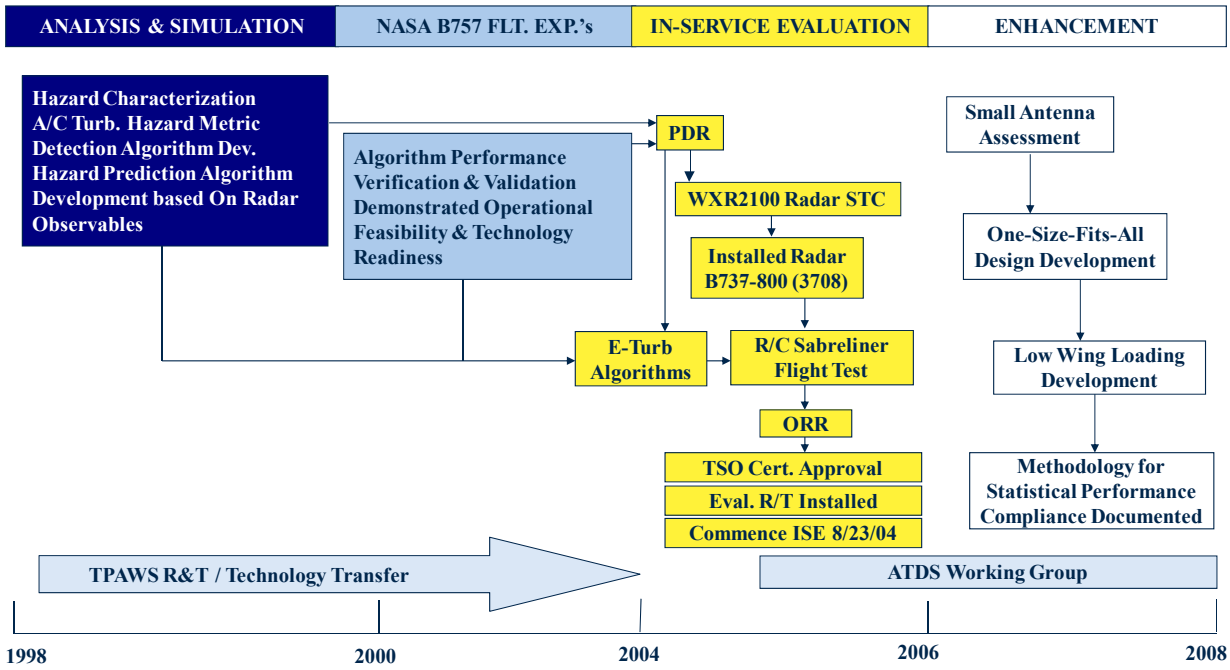

Figure 1: Timeline of NASA Sponsored E-Turb Radar Research and Development

Several avionics manufacturers are currently developing forward-looking turbulence detection systems for commercial aircraft using new airborne pulse Doppler radar technology. The difficulty in evaluating these systems under realistic hazardous turbulence and operational conditions has raised new certification issues. A significant part of the certification process will require estimating system performance using a combination of analytical studies, computer simulations, and flight tests.

In order to facilitate the certification process, the Federal Aviation Administration (FAA) formed and is leading an Airborne Turbulence Detection System (ATDS) Working Group inclusive of NASA, AeroTech Research, Rockwell Collins, Honeywell, Boeing, and Airbus personnel to determine the Minimum Operational Performance Standards (MOPS) and establish the certification methodology. In the proposed certification requirements as documented by the FAA in the ATDS Working Group's MOPS, minimum probabilities of missed and false turbulence indications have been specified. Each manufacturer seeking FAA certification approval for a specific aircraft application must make estimates of these probabilities for one of the three aircraft classes as defined in FAA Technical Standard Order (TSO) C134 (Reference [2]). The ATDS Working Group and the FAA established a three aircraft class differentiation based on wing loading criteria (aircraft weight divided by wing reference area). The specific classes are defined as:

- Class A – 80 to 135 lbs/ft^2
- Class B – 60 to 100 lbs/ft^2
- Class C – 30 to 70 lbs/ft^2

The methodology and examples presented in this document focus on the Class A (large transport category aircraft), but results are applicable to the other two classes of aircraft. In the following sections, algorithms used for estimating turbulence hazards from basic radar measurements are described and a methodology for estimating probabilities of missed and false turbulence indications under noise limited conditions is presented. This end-to-end methodology includes the formulation, development, and verification of the necessary governing equations and computational tools to calculate probabilistic detection performance for g-based turbulence prediction systems employing airborne radar observables. The formulation considers aircraft characteristics and associated errors as well as airborne radar measurement characteristics and detection errors. Overall end-to-end statistical performance of the g-based turbulence system depends, in general, on the product of two random variables and the individual statistical characteristics of both random variables. Although the methodology described herein is specific to the detection techniques and algorithms used, it serves as a guide for calculations on other systems proposed for certification by various manufacturers of radar based turbulence detection systems.

2. Aircraft Centric Turbulence Hazard Metric Definition

Early in the NASA TPAWS Program, there was an effort to identify a metric which quantifies a turbulence hazard to a commercial transport aircraft. The primary requirements were:

1. It should unambiguously represent the intensity of the turbulence hazard based on accelerations, which result in injuries and damage to an aircraft.
2. It should not depend on the atmospheric phenomenon that produces the effect on the aircraft.
3. It could be related to measurements or observables made by various forward-looking airborne sensors (e.g., radar, lidar, etc.).
4. It could be measured by in situ sensors onboard an aircraft; thereby, providing a "truth" measurement to assess the performance of the forward-looking sensors.
5. It could be readily scaled from one aircraft to another based on accepted physics. (Reference [3])

The metric that best satisfies these conditions was a running 5-second windowed root mean square (RMS) of the aircraft vertical acceleration, denoted by $\sigma_{\Delta n}$. The metric was refined in simulations and several sets of flight experiments on NASA's B757-200 research aircraft under TPAWS. There is plausible justification for this choice of metric given the longitudinal response characteristics and operating speeds of transport category aircraft. The selection of five seconds was based on two key considerations:

- The need to balance between 1) a sample window small enough to adequately resolve small scale turbulence that affect aircraft through induced g-loads and 2) an accelerometer measurement sample size large enough to calculate an RMS with acceptably small random error; and
- Five seconds corresponds to the one-kilometer spatial average used for the airborne radar turbulence signal processing, based on typical cruise airspeeds. Therefore, there was consistency between the forward-looking airborne sensor and the in situ accelerometer measurements.

The $\sigma_{\Delta n}$ parameter can also be related to the peak accelerations experienced by an aircraft. Figure 2 shows turbulence encounters from historical flight data; including data collected during previous NASA flight tests, the E-Turb Radar In-Service Evaluation, National Transportation and Safety Board (NTSB) accident investigations, and several other airline incidents and accidents. A linear regression applied to this data yields a correlation of 95%. This data clearly demonstrates that the $\sigma_{\Delta n}$ parameter can be used as a surrogate for peak loads.

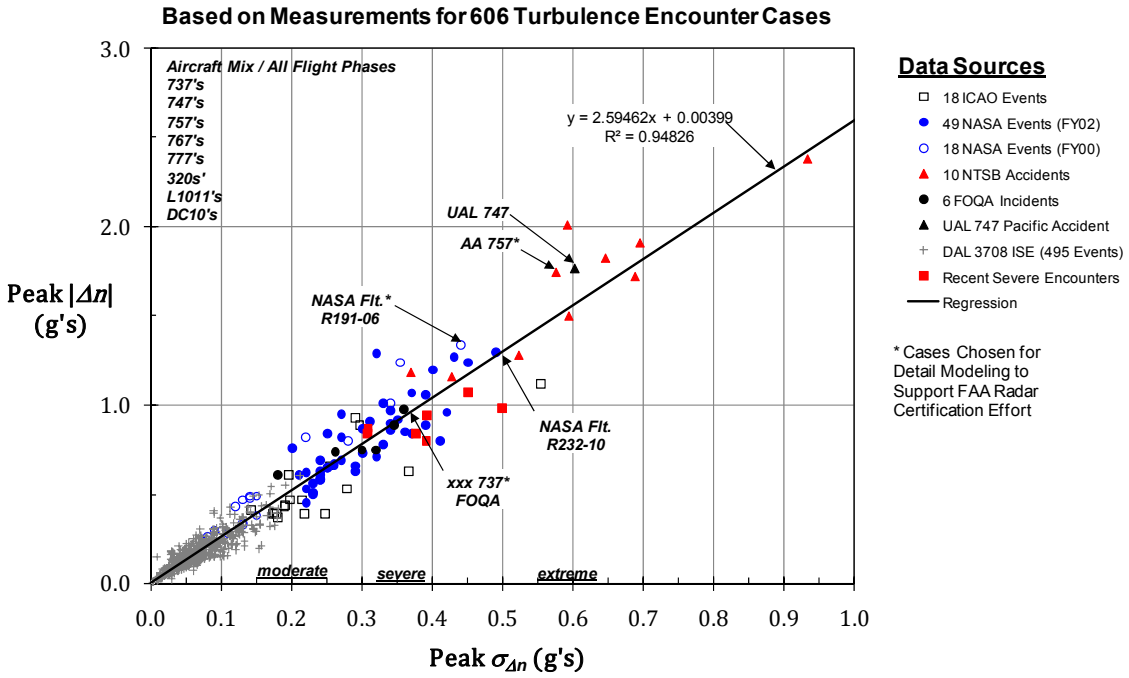

Figure 2: Correlation between Peak Load and Peak $\sigma_{\Delta n}$ (5 sec. window)

Analyses were conducted to select thresholds of $\sigma_{\Delta n}$ that could be used to define the various levels of turbulence intensity. The selection of thresholds was hampered by the lack of clear, objective data relating the $\sigma_{\Delta n}$ parameter to the usual subjective descriptions of light, moderate, and severe turbulence. The FAA Aeronautical Information Manual (AIM) states that during severe turbulence "occupants are forced violently against seat belts …" and/or "the aircraft may be momentarily out of control." Based on this, a threshold of $\sigma_{\Delta n} = 0.3$g was conservatively chosen as the lower limit of severe turbulence. These data are consistent with thresholds defined in the Forecasting Guide on Turbulence Intensity (Reference [4]). The FAA in TSO-C134 has specified the g-based metric for representing enhanced turbulence predictions based on radar observables.

It is important to note that no scientific basis exists to be exact in the categorizations of the turbulence intensities. The exact subjective assessment of turbulence is controversial and has not been definitively determined. The turbulence metric thresholds selected can be used as a basis for warning pilots and dispatchers of potential safety hazards. The following categorization was adopted for the E-Turb Radar analysis within this report.

$\sigma_{\Delta n} \leq 0.1$g	Light Turbulence
$0.1 < \sigma_{\Delta n} \leq 0.2$g	Moderate Turbulence
$0.2 \leq \sigma_{\Delta n} < 0.3$g	Moderate to Severe Turbulence
$0.3 \leq \sigma_{\Delta n} < 0.6$g	Severe Turbulence
$0.6 \leq \sigma_{\Delta n}$	Extreme Turbulence

3. Hazard Prediction Algorithm Design

As discussed in Section 2, the overall turbulence hazard to an aircraft is characterized by a numerical value (g-units) of RMS vertical acceleration excursions relative to 1g quiescent flight. This metric predicts impending impact on an aircraft and its occupants as well as unacceptable flight path excursions, and is based on accepted fundamentals of flight mechanics. Using these fundamental concepts, the quantitative impact of turbulence on an aircraft can be mathematically defined.

Aircraft respond to lift changes induced by deviations of angle of attack, which result from atmospheric velocity disturbances. Such lift changes produce aircraft loads, which are proportional to point variance of the turbulence velocity field. In order to predict aircraft loads based on radar observables, a relationship between the radar spectrum width measurement, point variance of turbulence intensity, and $\sigma_{\Delta n}$ is needed. Such a relationship, based on the physics of the radar measurement process, allows estimation of turbulence point variance from radar observables. The structure of a generic hazard prediction algorithm based on airborne radar observables can be approximated by:

$$\hat{\sigma}_{\Delta n} = \left[\frac{\sigma_{\Delta n}}{unit\ \sigma_{\mathrm{w}}}\right]_{table} \cdot \frac{[\bar{M}_2(\vec{x})]^{0.5}}{\frac{\sqrt{\langle\sigma_v^2(r)\rangle}}{\sigma}} \tag{1}$$

where:

$\hat{\sigma}_{\Delta n}$ = Predicted value of RMS vertical load excursion from 1g (g's)

$\left[\frac{\sigma_{\Delta n}}{unit\ \sigma_{\mathrm{w}}}\right]_{table}$ = Aircraft scale (conversion) factor (g's/m/s)

$\bar{M}_2(\vec{x})$ = Radar 2nd moment / spectrum width product (m^2/s^2)

$\sqrt{\langle\sigma_v^2(r)\rangle}/\sigma$ = Radar pulse volume compensation factor based on theory (non-dimensional)

In the above equation, σ_w is defined as the standard deviation of the vertical component of the turbulent wind field and σ is the RMS intensity of the turbulent wind field based on one-dimensional von Kármán energy spectra. A specific point in radar range-azimuth space is defined by $\vec{x}$. It is assumed that σ provides a close approximation for the standard deviation of the component of the turbulent wind field in the horizontal direction (σ_u) as viewed along a radar radial. For evaluation of system performance, an acceptable assumption is that $\sigma_w \approx \sigma_u$. This local isotropy assumption, when considering the physical dimensions of the radar resolution volume, is further justified by analysis of NASA flight test data found in Reference [5].

The aircraft-scaling factor in general depends on aircraft altitude, airspeed, and weight. When considering conversion of radar measurement products to aircraft load prediction, two distinct cases may be implemented. The first case directly applies existing turbulence hazard table data developed under NASA sponsorship (see Section 6). Data exists for a variety of aircraft types ranging from A320-200 to B747-400 for altitudes of 5,000 feet to service ceilings, over the entire operational weight range for each aircraft. This system implementation requires aircraft weight to be interfaced to the radar and is referred to as the "weight strapped" configuration. The design philosophy for the second case seeks to remove weight (wing loading) dependence while achieving an acceptable error budget, thus reducing overall system cost and implementation complexity. For this case, a statistical algorithm design is required for the g-based turbulence system consistent with the design criteria that aircraft weight shall not be "strapped" to the radar system. This notion has been referred to as the "one-size-fits-all" system configuration. Further details of the "one-size-fits-all" approach including relevant data for application is discussed in Section 6 and 7 of this report.

If an applicant seeking certification approval elects to include radar pulse volume compensation for their system implementation, then such considerations should be included when demonstrating compliance to performance required in sections 1.3(a) and 1.3(b) of the ATDS Working Group's MOPS. The performance criteria documented in this MOPS was based on a consensus formed over several years by the ATDS Working Group. The technical necessity for this compensation factor stems from the fact that spatial spectra of turbulence velocities are filtered by the radar resolution volume characteristics (for specific radar & antenna design parameters) and thus produces attenuation in observed turbulence intensity estimates derived from radar measurements. This phenomena is referred to as pulse volume filtering, the physics of which describe how turbulent kinetic energy is partitioned between subresolution

volume scales and scales larger than the radar resolution volume. In effect, a radar system acts as a high pass filter measurement device. The key determinant is the pass band of the filter process, which is a function of the specific radar performance characteristics and configuration considered. The filtering impact is more pronounced for larger antennas than smaller antenna systems. The governing equations for calculating the compensation factor including representative numerical results for selected radar parameters are presented in Appendix I. The compensation factor is range dependent and is approximately equal to unity at longer ranges and decreases as range decreases.

For purposes of simplicity and clarity of notation in the subsequent text, the following definitions are introduced:

z = RMS predicted vertical load from 1g reference (g's)

x = Aircraft scaling (conversion) factor (g's/m/s)

y = Radar 2nd moment/spectrum width product (m/s)

k = 1/ pulse volume compensation factor (non-dimensional)

Considering the revised nomenclature, Figure 3 shows a diagram of the E-Turb Radar system concept. Real-time values of aircraft altitude, airspeed, and weight (if "strapped") are used in the hazard prediction algorithm to scale the 2nd moment/ spectrum width to a predicted $\sigma_{\Delta n}$. The 2nd moment measurement and predicted load products are available as a function of range and azimuth over the scanning domain of the radar antenna and (i, j) designates a specific range-azimuth intersection.

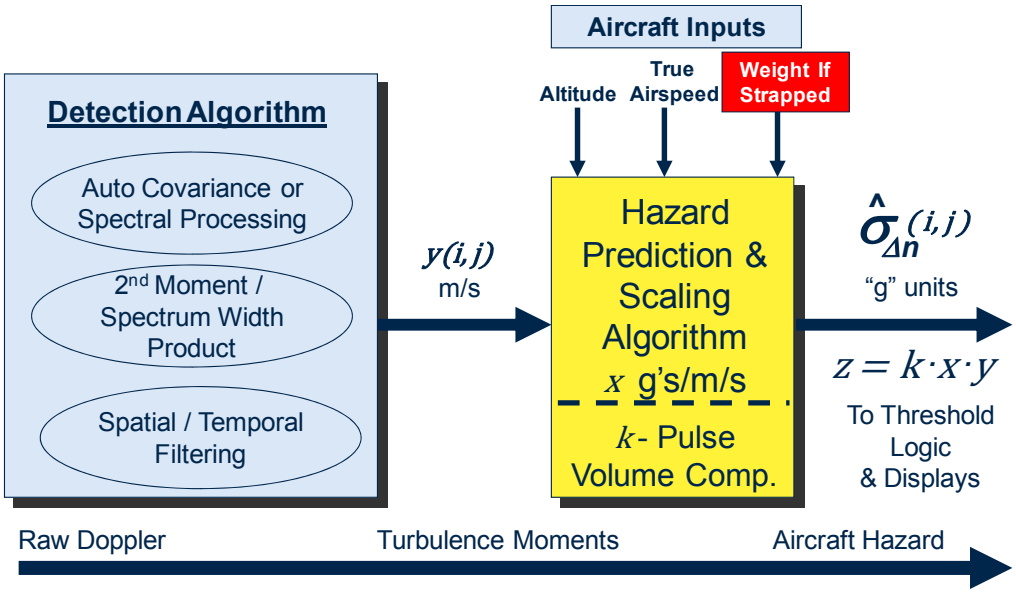

Figure 3: E-Turb Radar System Concept

4. Probability Calculations

The key objective of the material presented in this section is to formulate, develop, and provide initial verification of the necessary governing equations and computational tools to establish probabilistic detection performance for g-based turbulence prediction systems employing airborne radar observables. The formulation considers aircraft characteristics and associated errors (x-component) as well as airborne radar measurement characteristics and detection errors (y-component). The aircraft turbulence induced load conversion factor, x, has units of g's/m/s and the radar spectrum width estimate, y, has units of m/s. Overall end-to-end statistical performance ($z = kxy$ in units of g) of the g-based turbulence system

depends on the product of two random variables and the individual statistical characteristics of both the x and y random variables. The developed methodology, which is consistent with the requirements of the ATDS Working Group's MOPS, as well as the governing equations for system performance hypothesis testing including initial results, was presented at the FAA-ATDS workshops held in March and August of 2007. The material presented at the workshops included a method for determining the turbulence system cockpit display threshold, consistent with realistic nuisance and must detect/indicate probabilities.

4.1 Formulation of Governing Equations

Consider the random variable $z = xy$ where x and y are positive random variables and assumed independent with a joint density function $f(x,y) = f_x(x)f_y(y)$. The x and y random variables and their associated probability density functions (PDF) are restricted by physics to $x \geq 0$ and $y \geq 0$. It is assumed that the radar spectrum width has been pulse volume compensated. Explicit modification of the equations found herein for inclusion of pulse volume compensation is provided in Appendix II. The objective is to calculate the PDF, the cumulative distribution function (CDF), and the first three moments of the random variable z given the process $z = xy$. Based on accepted fundamentals of probability theory (Reference [6]), the CDF and PDF of z for any random outcome ζ are defined respectively as:

$$F_z(z) = \Pr(\zeta \leq z) = \iint_{D(z)} f(x,y)dxdy \tag{2}$$

$$p_z(\mathrm{z}|\mathrm{z} \geq 0)dz = \iint_{\Delta D(z)} f(x,y)dxdy \tag{3}$$

Where the region $D(z)$ is the region in the $x-y$ plane bounded by the hyperbola $z = xy$ for fixed positive values of z and the $+x$ and $+y$ axes. This region lies in the first quadrant of the $x-y$ plane and is characterized by the condition $x < z/y$ for fixed non-zero positive values of z. The region $\Delta D(z)$ is defined such that $z < xy < z + dz$ is the region bounded by the hyperbola's $x < z/y$ and $x < (z + dz)/\,y$. The coordinates of a point in this region are $(z/y, y)$ and the area of a differential equals $dydz/y$. For the conditions and definitions stated above we obtain:

$$F_z(z) = \Pr(\zeta \leq z) = \int_0^\infty f_y(y) \int_0^{z/y} f_x(x)dxdy \tag{4}$$

$$\therefore\ F_z(z) = \int_0^\infty f_y(y)\, G(z/y)dy \tag{5}$$

The probability density function of z can be found by appropriate integration over the region $\Delta D(z)$ or by differentiating the cumulative distribution function of Equation (4) with respect to z. Therefore:

$$p_z(\mathrm{z}|\mathrm{z} \geq 0) = \frac{dF_z(z)}{dz} = N\int_0^\infty f_y(y)\frac{dG(z/y)}{dz}dy = N\int_0^\infty \frac{f_y(y)f_x(z/y)}{y}dy \tag{6}$$

Where N is defined as a normalization factor such that $\int_0^\infty dF_z(z) = 1$. Analysis of Equations (5) and (6) shows that:

$$F_z(z) \text{ increases monotonically as a function of } z \text{ for } 0 \leq z \leq \infty \tag{7}$$

$$N = \frac{1}{1 - F_z(0)} \tag{8}$$

$$F_z(\infty) = 1 \tag{9}$$

$$\int_0^\infty p_z(\mathrm{z}|\mathrm{z} \geq 0)dz = 1 \tag{10}$$

$$p_z(\mathrm{z}|\mathrm{z} \geq 0) \geq 0 \tag{11}$$

$$\Pr(z_1 \leq \zeta < z_2) = \int_{z_1}^{z_2} p_z\,(\mathrm{z}|\mathrm{z} \geq 0)dz \tag{12}$$

Probability theory requires all the above properties to be true in order that the z cumulative distribution function and related probability density function produce legitimate statistics for the $z = xy$ random process. It should be noted that all the above integrals should be interpreted as Stieltjes integrals (Reference [6]), which admits a finite or denumerable number of discontinuities and impulses in the integrands. This is required for all probability to lie on the positive z-axis, since radar pulse pair estimators of spectrum width can return negative or zero values and $F_z(0)$ may not be zero.

Conventionally defined statistics for mean and variance can be calculated once the z-PDF as given by Equation (6) is known:

$$\mu_z = \int_0^\infty z p_z(\mathrm{z}|\mathrm{z} \geq 0)dz = N\mu_x\mu_y \tag{13}$$

$$\sigma_z^2 = \int_0^\infty z^2 p_z(\mathrm{z}|\mathrm{z} \geq 0)dz - \mu_z^2 = N^2\left[\left(\sigma_x\sigma_y\right)^2 + \left(\mu_x\sigma_y\right)^2 + \left(\mu_y\sigma_x\right)^2\right] \tag{14}$$

The μ's represent the means for the x and y random variables and the σ's are the standard deviations of x and y respectively.

Three different approaches have been used to derive the above results with complete agreement between the methods. The authors believe the formulation outlined above offers computational advantages. In order to verify the above equations, several Monte-Carlo simulations of the above process have been conducted, with excellent agreement between theoretical and simulation results. Some results and comparisons between theory and simulation are shown in the following sections.

4.2 Verification of Equation (5) and Equation (6)

4.2.1 Conditions Defined for Monte-Carlo Simulation

Aircraft flight conditions (i.e. $h = 10{,}000$ ft, airspeed = 250-290 kias) were selected for Class A aircraft systems and 20,000 operational sorties were simulated. The "one-size-fits-all" algorithm concept was assumed and statistical uncertainties in x are due to the fact that for each simulated operation the particular x-value was randomly selected from a distribution derived from aircraft operational weight data. The "one-size-fits-all" design value for x is based on a reference wing loading and varies as a function of altitude and speed. Specific x-parameters are: (see Figure 8)

$$\mu_x = 0.04662 \text{ g/m/s} \tag{15}$$

$$\sigma_x = 0.004256 \text{ g/m/s} \tag{16}$$

$$\text{Note: } \sigma_x\mathrm{error}/\mu_x \approx 0.1 \tag{17}$$

Given that a Gaussian distribution closely approximates the x-distribution, for purposes of simulation we assume:

$$x \text{ random variable is } N(\mu_x, \sigma_x) \tag{18}$$

$$f_x(x) = \frac{1}{\sqrt{2\pi}\sigma_x} exp\left(-\frac{(x-\mu_x)^2}{2(\sigma_x)^2}\right) \tag{19}$$

4.2.2 Radar y-Component of Hazard Algorithm

For purposes of simulation and insufficient specific information from the ATDS industry team, the following assumptions are made. Specific y parameters for the radar 2nd moment observable (spectrum width) are:

$$\mu_y = 5 \text{ m/s} \tag{20}$$

$$\sigma_y = 1 \text{ m/s} \tag{21}$$

$$\text{Note: } \sigma_y/\mu_y \approx 0.2 \tag{22}$$

The parameters chosen above are indicative of a relatively high radar signal-to-noise ratio (SNR). The specific form of the radar y probability density function will play a critical role in establishing a suitable system threshold for z and in assigning probabilities to nuisance and must detect/indicate requirements. For simulation purposes the following assumptions are made:

$$y \text{ random variable is } N(\mu_y, \sigma_y) \tag{23}$$

$$f_y(y) = \frac{1}{\sqrt{2\pi}\sigma_y} exp\left(-\frac{(y-\mu_y)^2}{2(\sigma_y)^2}\right) \tag{24}$$

4.2.3 Monte-Carlo Simulation Results

Given the terms of reference as stipulated above (both theory and simulation), a comparison of theoretical (calculated from Equations (5) and (6)) and Monte-Carlo simulation results are shown in Figure 4 and Figure 5.

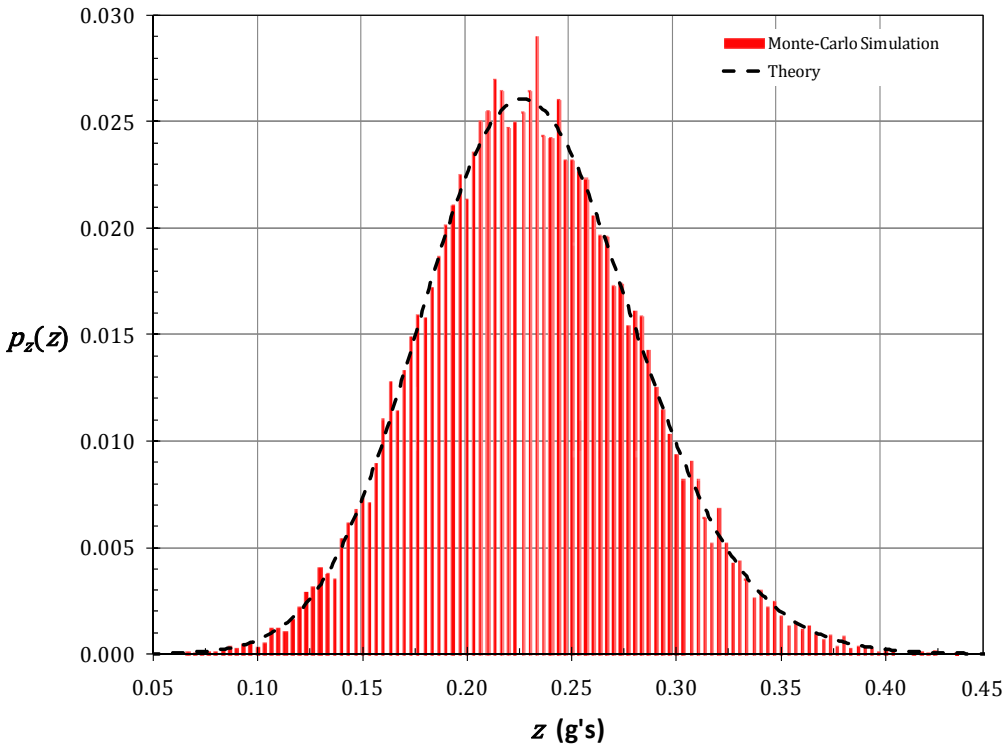

Figure 4: PDF Comparison for 20,000 Flight Operations

Table 1: Comparison of z Statistics

Measure	Simulation	Theory
Zeroth Moment	1.0	1.0
Mean	0.23329 g's	0.23131 g's
Standard Deviation	0.05139 g's	0.05142 g's

Comparison of the cumulative probability distribution functions is shown in Figure 5.

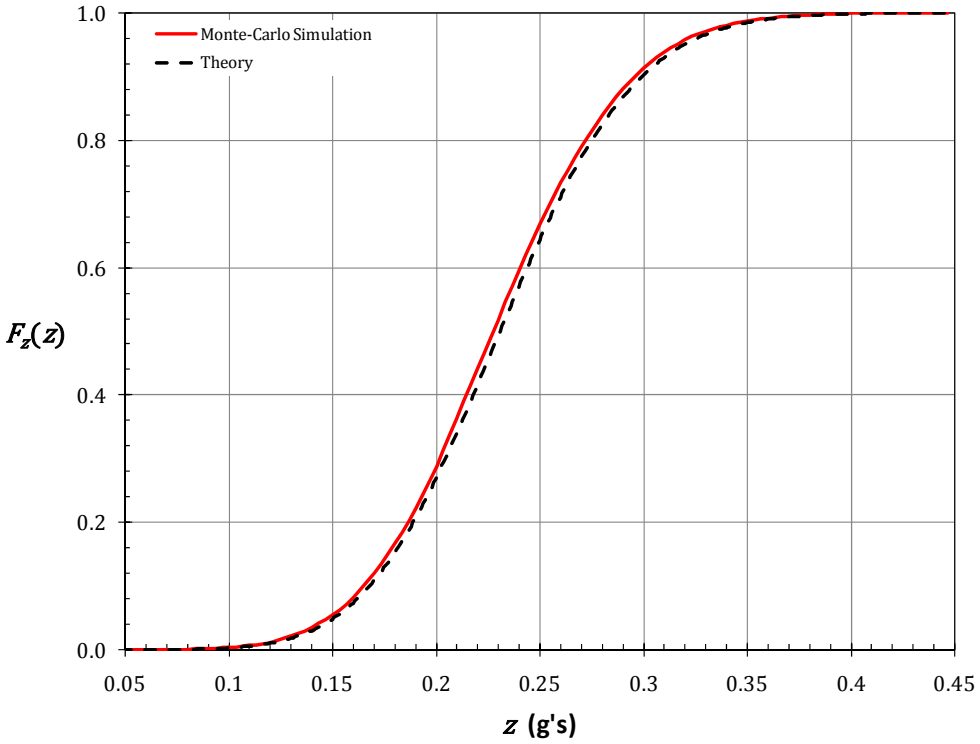

Figure 5: CDF Comparison for 20,000 Flight Operations

The comparisons shown between Monte-Carlo simulation and calculated results based on Equations (5) and (6) provide convincing evidence as to the validity of the governing equations as developed above.

4.2.4 Aircraft Weight "Strapped" Condition

Reduction of the z-PDF (Equation (6)) for the case where aircraft weight is "strapped" to the radar is developed below. For this case, the x-PDF is characterized by the Dirac delta function such that the following are true:

$$f_x(x) = \delta(x - x^0); \quad \int_0^\infty f_x(x)dx = 1 \tag{25}$$

$$\mu_x = x^0; \quad \sigma_x = 0 \tag{26}$$

The variable x^0 represents a particular aircraft hazard table point-set value which in general depends on aircraft type, speed, altitude, and weight. These tables were developed under NASA contract, and documentation describing their development and use is presented in Section 6. For the case considered, Equation (6) takes the following form:

$$p_z(\mathrm{z}|\mathrm{z} \geq 0) = \frac{1}{1-F_z(0)} \int_0^\infty \frac{f_y(y)\delta\left(\frac{z}{y} - x^0\right)}{y} dy \tag{27}$$

For evaluation of the integral as defined by Equation (27), it is convenient to use the following property associated with Dirac delta functions

$$\int_a^b h(t)\delta\big(g(t)\big)dt = \frac{h(t^0)}{|g'(t^0)|} \tag{28}$$

provided $g(t) = 0$ has a single root t^0 in the interval $a < t < b$. Examining Equation (27) we conclude $g(y) = z/y - x^0$ with a single root at $y^0 = z/x^0$ for fixed positive values for z and x^0**.** The derivative of $g(y)$ evaluated at y^0 is $(x^0)^2/z$; therefore evaluating Equation (27) yields:

$$p_z(\mathrm{z}|\mathrm{z} \geq 0) = \frac{1}{x^0(1-F_y(0))} f_y\left(\frac{z}{x^0}\right) \tag{29}$$

Although the above result is well known in the case where x is deterministic, it is instructive to derive the result from the more general equation involving the product of two random variables, which is the case relevant to the turbulence radar for the "one-size-fits-all" algorithm design. If the y-PDF is Gaussian as assumed in the above numerical calculations, Equation (29) reduces to:

$$p_z(\mathrm{z}|\mathrm{z} \geq 0) = \frac{N}{\sqrt{2\pi}x^0\sigma_y} exp\left(-\frac{(z-x^0\mu_y)^2}{2(x^0\sigma_y)^2}\right) \tag{30}$$

where the mean and standard deviation of z is:

$$\mu_z = Nx^0\mu_y \tag{31}$$

$$\sigma_z = Nx^0\sigma_y \tag{32}$$

Results have been calculated comparing the "one-size-fits-all" algorithm statistical design philosophy to a weight "strapped" implementation. Results of this analysis have been presented to the FAA-ATDS working group. The overall end-to-end methodology for calculating the must detect/indicate and must not indicate/nuisance probabilities as required by the ATDS Working Group's MOPS, with application to specific Class A aircraft systems and flight conditions, is shown in Section 9 of this report.

5. Calculation of Nuisance and Missed Detection Probabilities

Discussion of a probabilistic theoretic technique for calculation of must indicate and must not indicate probability is provided in this section. The technique discussed is based on accepted hypothesis testing methods and utilizes the basic equations developed in Section 4. E-Turb Radar pass/fail statistical performance criteria for Class A aircraft systems, as specified in sections 1.3(a) and 1.3(b) of the ATDS Working Group MOPS, requires consideration of two cases. Section 1.3(a) states that the radar shall indicate turbulence that corresponds to a $\sigma_{\Delta n}$ of 0.3g for weather targets with reflectivity greater than or equal to 20 dBZ at a minimum of 12 nautical miles with a probability of 0.85. Equivalently, the probability of not indicating a hazard (missed detection) must be less than 0.15. The second case, as defined in section 1.3(b), states that the radar shall not indicate turbulence that corresponds to a standard deviation of aircraft g-load excursions of 0.1g for weather targets with reflectivity greater than or equal to 20 dBZ at a minimum of 12 nautical miles with a probability of 0.20. Equivalently, the probability of not indicating a hazard must be greater than 0.80 for the second case. The basic concepts underlying the statistical theory of hypothesis testing are shown in Figure 6. The techniques discussed above are also applicable to Class B and C aircraft systems based on performance levels defined in FAA TSO-C134.

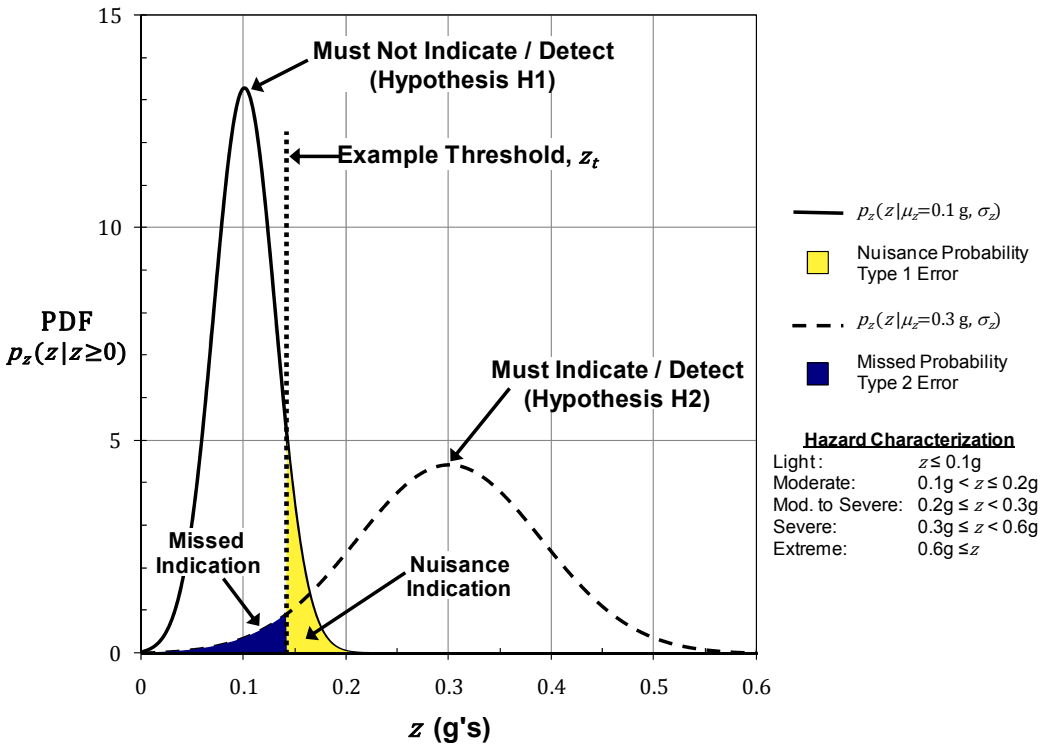

Figure 6: Calculation of Nuisance and Missed Detection Probabilities Based on Hypothesis Testing

As indicated in Figure 6, hypothesis H1 defines the must not indicate/detect conditions and H2 defines the must indicate/detect requirement. A representative example threshold (z_t) for z is also shown in Figure 6. It should be noted that regardless of where the threshold is placed, an error of Type 1 (nuisance) or Type 2 (missed), or both, will occur. The area under the z-PDF (dashed line) to the left of the example threshold is the probability of missed detection (i.e. no indication of turbulence) when in fact hypothesis H2 is true. The ATDS Working Group's MOPS requirement is that this estimate should not exceed 0.15. Likewise the area under the z-PDF (solid curve) to the right of the example threshold is the probability of a nuisance detection (i.e. indication of turbulence) when in fact hypothesis H1 is true. In this case, the requirement of the MOPS is that this estimate should not exceed 0.20. The z-PDF curves shown in Figure 6 were computed using Equation (6) developed in Section 4 of this report. The z-PDF's shown were based on the "one-size-fits-all" model and published radar performance data that will be further discussed in Sections 6 and 8 of this report respectively. It should be noted, that although the probability density functions shown in Figure 6 appear to be Gaussian, in fact they are not. In general, the random variable $z = xy$ is not Gaussian, even in the case where the random variables x and y are both Gaussian.

In order to calculate probabilities defined above, the PDF of the random variable z must first be calculated using Equation (6), previously developed in Section 4. Once the z-PDF is known for $0 \leq z \leq \infty$, the probability of a nuisance turbulence indication can be calculated using the following equation:

$$\Pr(z \geq z_t) = \int_{z_t}^{\infty} p_z(z|z \geq 0, \mu_z = 0.1\text{g}, \sigma_z)dz \tag{33}$$

Likewise the probability of a correct turbulence indication can be calculated:

$$\Pr(z \geq z_t) = \int_{z_t}^{\infty} p_z(z|z \geq 0, \mu_z = 0.3\text{g}, \sigma_z)dz \tag{34}$$

The probability of a missed turbulence indication is the complement of Equation (34).

Equation (13) may be used to set the 0.1g and 0.3g conditions as defined in the integrands of Equations (33) and (34) respectively. If the mean of the aircraft conversion factor x is known as a function of flight conditions (see Section 6), then the mean of the radar spectrum width y can be calculated from Equation (13) such that the 0.1g and 0.3g design conditions are true. For example, if the mean of x is assumed to be the value used in the verification analysis of Section 4, then the mean of y (y is assumed to have been pulse volume compensated) required to achieve the 0.3g must indicate condition, assuming the normalization factor $N = 1$, is given by:

$$\mu_y = \frac{0.3\text{g}}{0.04662\ \text{g/m/s}} = 6.435\ \text{m/s} \tag{35}$$

The variance of y is the key parameter in determining the end-to-end performance characteristics of an E-Turb Radar system. The variance of y is a function of spectrum width estimator properties and specific spatial and temporal averaging techniques employed by the applicant.

6. Technical Approach for Hazard Table Generation and "One-Size-Fits-All" Model for Class A Aircraft Systems

As discussed in previous sections, the ATDS Working Group's MOPS requires conversion of airborne radar measurement products to estimated RMS g-loads. Conversion of radar spectrum width to RMS g's is dependent on aircraft gust load response characteristics. Aircraft gust load response characteristics may be described by hazard table data, which is a function of aircraft weight and balance, airspeed, and altitude.

The technical approach for the generation of the hazard table for a group of aircraft of similar design is presented in Figure 7. The first five boxes of the table are specific to each contributing aircraft of the final hazard table product and are labeled as "weight strapped." The approach taken in this body of work addresses the generation of one hazard table for one class of aircraft that can be estimated from a baseline set of statistical data. The following describes, in further general detail, each of the contributing parts of Figure 7.

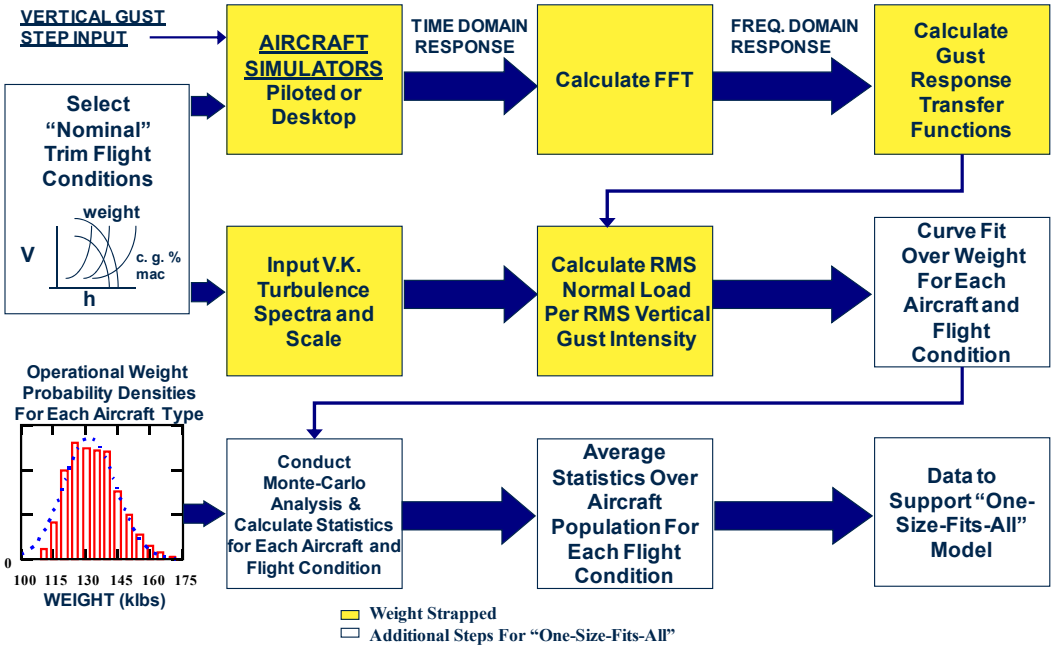

Figure 7: Technical Approach for Hazard Table Generation and "One-Size-Fits-All" Model for Class A Aircraft Systems

The data collection process begins with the definition of the trim flight conditions of interest for a specific aircraft type. The selected conditions focus on the operational flight envelope of the commercial aircraft of interest in terms of altitude (typically 5,000 to 40,000 feet), weight (typically operating empty weight to maximum gross weight), and center of gravity position (a percentage of mean aerodynamic chord for the aircraft type). Gust penetration airspeed or Mach number is selected for each altitude and weight condition considered. The selection process of these flight conditions is done in partnership with the Original Equipment Manufacturer (OEM), simulator personnel, and project personnel.

The next key step is the selection of the source for the aircraft response data that will be the primary input into the hazard table generation. Previous data collection processes focused on the Level D, FAA certified, Full-Flight Simulators available at many larger commercial carrier training facilities or NASA research centers. These simulators (Reference [7]) provide the highest level of fidelity in matching the real-world aircraft, including its response to a turbulence gust and the modeling of the ship's auto-pilot response to disturbances. Suitable data may also be collected from "desktop" simulators if the same level of fidelity is present within the dynamic response model. The benefit of using a desktop simulator versus a piloted simulator is the speed at which the data collection process can be accomplished and the cost savings associated with this option.

After a suitable simulator has been selected that meets the needs and requirements of the data collection team, data is collected from the simulator by the project team and simulator management personnel that will be used in the formation of the hazard table. A data collection matrix is developed from the identified trim flight conditions focusing on a range of altitudes, weights, and c.g. positions. The input disturbance to the simulator is a vertical gust in the inertial axis of the system with no other ambient atmospheric phenomenon present. This isolates the computer's calculated aircraft response to the gust input, the kernel of the aircraft response needed in the hazard table generation. For each point within the data collection matrix, a time series response of the aircraft to this gust input is calculated by the aircraft simulator model and stored for offline data processing.

Once the recorded data has been processed and checked for such anomalies as poor trim conditions, unsteady flight conditions after the disturbance or noisy signals in general, the data is reduced into a subset of the total time response, isolating only the aircraft's response to the turbulence input. In general, significantly more data is collected in each run for diagnostic purposes. A Fast Fourier Transform (FFT) is applied at each data point from the data collection matrix for the normal acceleration and the inertial vertical gust time series' response, thereby transforming them into a frequency domain response for the specific flight conditions.

With the individual frequency responses for each resulting time series for each individual data collection point in hand, the gust response transfer function is now calculated. This provides the basic information required for the eventual generation of a hazard table.

To calculate the RMS normal load per RMS vertical gust velocity response, a calculation is performed that combines the frequency response gust transfer functions with the modeled von Karman turbulence spectra. The von Karman spectra and associated scale lengths (20 to 2000 meters) are calculated based on the flight conditions for each of the data collection points. The resulting product of RMS normal load per RMS vertical gust velocity is in the units of g's/m/s. A table of values for the range of length scales is generated for each aircraft type of interest. A default turbulence length scale of 500 meters is recommended for application of the hazard table data.

The approach outlined above has been successfully applied to eight commercial transport category aircraft (Class A) ranging in size from a B737-300 to a B747-400. The format of the hazard table data for one selected commercial transport aircraft is shown in Table 2. The dash marks within Table 2 represent flight conditions for which a suitable trim solution was not possible for this particular aircraft, altitude, weight, and center of gravity position.

Table 2: Example Format and Data for a Hazard Table for a Commercial Transport Aircraft (Class A)

Weight (klbs)	Altitude (kft)							
	5	10	15	20	25	30	35	40
100	0.05423	0.05742	0.05400	0.05071	0.05227	0.05432	0.05100	0.04501
110	0.05109	0.05341	0.05036	0.04718	0.04945	0.05260	0.04970	0.04204
120	0.04650	0.05072	0.04755	0.04474	0.04532	0.04958	0.04624	0.03640
130	0.04295	0.04795	0.04463	0.04258	0.04141	0.04632	0.04165	0.03185
140	0.03925	0.04428	0.04174	0.04035	0.03821	0.04425	0.03796	0.03049
150	0.03621	0.04058	0.03869	0.03826	0.03515	0.04188	0.03506	-
160	0.03417	0.03638	0.03550	0.03737	0.03346	0.03976	0.03096	-
170	0.03264	0.03196	0.03274	0.03456	0.03299	0.03695	0.02834	-

The additional steps needed for the calculation of "one-size-fits-all" x-PDFs are indicated by the last four blocks in Figure 7. The hazard table data for each of the eight aircraft is used to obtain a functional curve fit over weight (wing loading) for each aircraft and flight condition (altitude and airspeed). Operational weight statistics for a variety of aircraft, provided by participating airlines and OEMs, is then used to define weight PDFs for each aircraft considered. Aircraft weight data for over 900,000 takeoffs and landings was used to statistically define the PDFs. Using the functional weight curve fit and weight PDFs, a Monte-Carlo analysis is conducted and relevant statistics are calculated for the x values (g's/m/s) for each aircraft and flight condition. Finally, the x values are averaged over the eight-aircraft population for each flight condition. The final data product for the "one-size-fits-all" design is a PDF of the conversion factor for radar second moment observables and is shown in Figure 8 in multiple graphs for the purpose of readability.

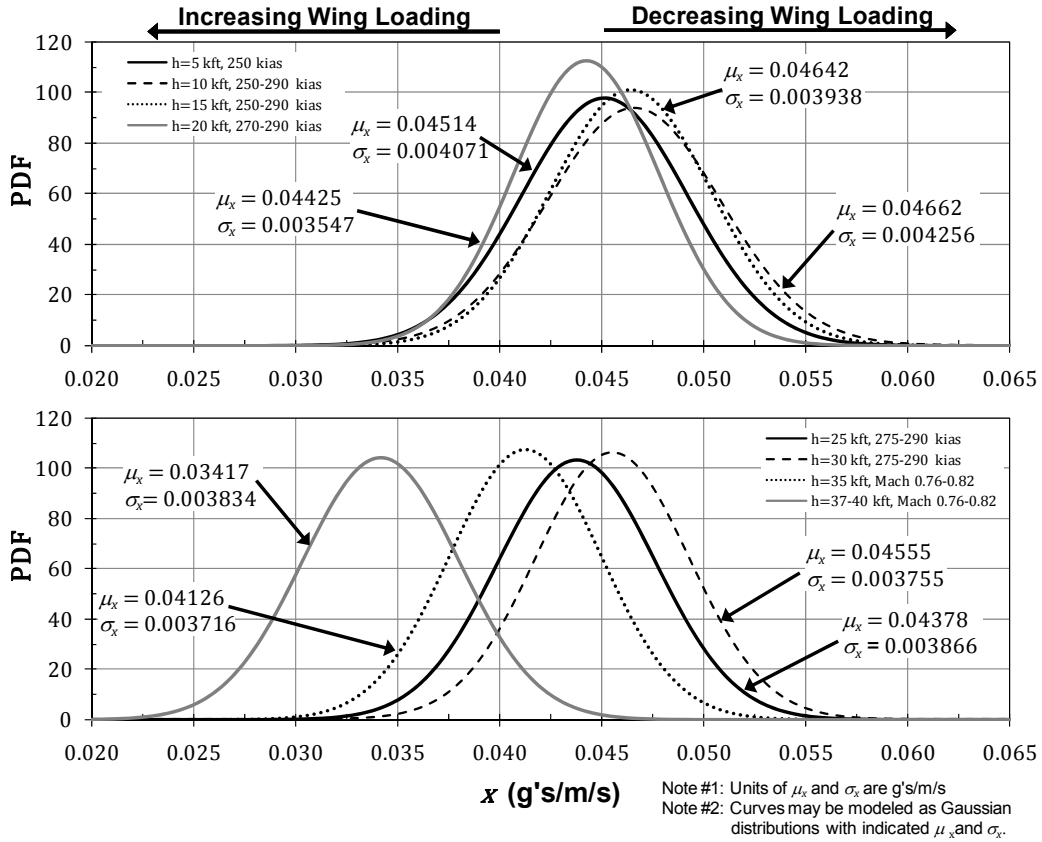

Figure 8: Class A Probability Density Functions for "One-Size-Fits-All" Algorithm Applicable for Aircraft Wing Loading between 80 and 135 lbs/ft^2

Table 3 lists the specific values for each flight condition present within the "one-size-fits-all" design for Class A aircraft systems.

Table 3: Class A Probability Density Functions for "One-Size-Fits-All" Algorithm Applicable for Aircraft Wing Loading between 80 and 135 lbs/ft^2

Flight Condition		PDF Conversion Factor	
Altitude (kft)	Airspeed (kias/Mach No.)	Mean, μ_x (g's/m/s)	Standard Deviation, σ_x (g's/m/s)
5	250	0.04514	0.004071
10	250-290	0.04662	0.004256
15	250-290	0.04642	0.003938
20	270-290	0.04425	0.003547
25	275-290	0.04378	0.003866
30	275-290	0.04555	0.003755
35	0.76-0.82	0.04126	0.003716
37-40	0.76-0.82	0.03417	0.003834

The curves shown in Figure 8 and the data listed in Table 3 may be modeled as Gaussian distributions with means and standard deviations as indicated for each flight condition. These probability density functions are acceptable for typical jet transport category airplanes with wing loading between 80 and 135 lbs/ft^2 throughout the entire flight regime. For turbulence systems intended for installation on non-typical aircraft with configurations or wing loading outside this range; the impact of configuration and wing loading must be considered when calculating the probability of missed detection and false positive turbulence indications.

7. Conversion Factor PDFs for Class B and C Aircraft Systems

As discussed in previous sections, the FAA TSO-C134 requires conversion of airborne radar measurement products to estimated RMS g-loads. The objective of this section is to extend and document the x-PDFs conversion factors to Class B and C aircraft systems as defined in FAA TSO-C134. The requirement for this extension stems from a FAA decision to provide a comprehensive TSO, applicable to a broad cross-section of aircraft types, including regional and business jets.

In order to extend conversion factors to Class B and C systems having wing loading characteristics lower than Class A, direct support from aircraft OEMs was sought. Several OEMs were contacted to explore their participation in providing required aircraft response data. Two aircraft manufacturers, who produce a wide variety of business and regional jet aircraft, agreed to participate in the effort. After discussion with the OEMs, nine aircraft models were selected for data acquisition, including six executive business jets and three regional transport category jets. The data collection process and subsequent data processing techniques employed are consistent with those described by the first five boxes shown in Figure 7 of this report. All aircraft selected are modern in-production aircraft or will be in production within approximately a year. Some salient technical characteristics of the aircraft selected are summarized in Table 4. Values presented in the table below are representative but not exact in all cases.

Table 4: Data Collected for Class B and C Aircraft Systems

Aircraft Type	Wing Area (ft^2)	Wing Span (ft)	Maximum Altitude (ft)	Maximum Speed	Wing Loading Range (lbs/ft^2)
Biz. Jet	225	40	41,000	M 0.6	30 – 40
Biz. Jet	525	60	47,000	M 0.8	35 – 55
Biz. Jet	525	60	51,000	M 0.9	45 – 65
Biz. Jet	675	80	45,000	M 0.8	45 – 70
Biz. Jet	1025	90	51,000	M 0.8	50 – 95
Reg. Jet	525	70	41,000	M 0.8	60 – 100
Reg. Jet	725	80	41,000	M 0.8	60 – 100
Reg. Jet	750	80	41,000	M 0.8	65 – 110
Biz. Jet	450	60	41,000	M 0.7	65 – 105

Biz. Jet = Executive Business Jet Reg. Jet = Regional Jet

Based on longitudinal dynamic response data provided by the participating aircraft OEMs, turbulence aircraft databases were generated over a representative range of altitudes, airspeeds, and weights for the nine aircraft considered. Although the quality of the database is considered good, it is limited as regards to development of a "one-size-fits-all" statistical model for Class B and C systems due to the small population of aircraft included in each Class. In order to mitigate the impact of the limited population of aircraft considered, an alternative approach was developed that enabled the application of the large statistical sample of data for Class A aircraft systems presented in Section 6 of this report. The functional block diagram shown in Figure 9 illustrates the general technical approach for scaling Class A data to Class B and C systems. In order to implement the process outlined in Figure 9 a scaling law is first required. Once the scaling law is determined, calculations are made to transform Class A PDF data to Class B and C systems specifications. Finally the scaled results for Class B and C systems can be compared to those calculated directly from the limited OEM provided data for verification.

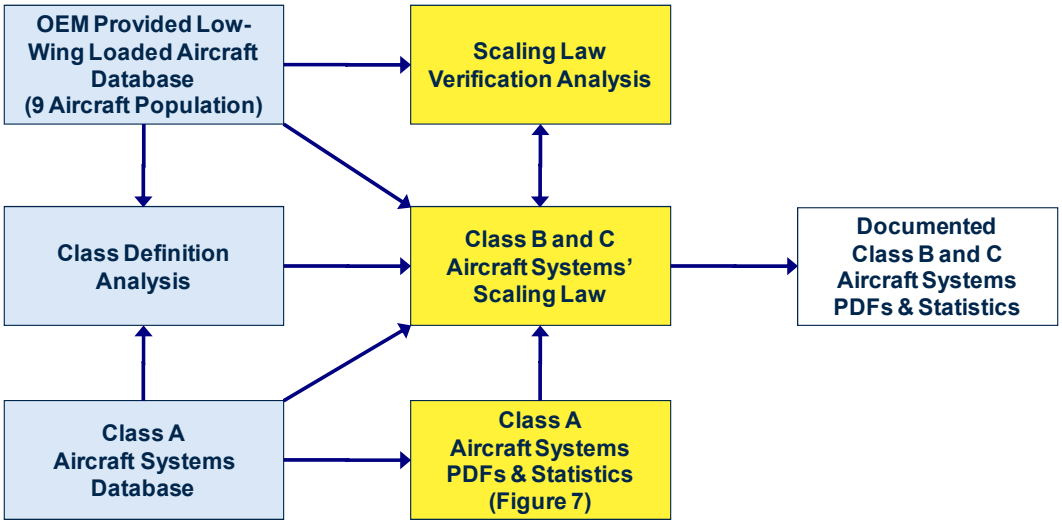

Figure 9: Technical Approach for Generating PDFs for Class B and C Aircraft Systems

The similarity scaling law derived is based on the well-known fact that the conversion factor x values (g's/m/s) are inversely proportional to wing loading and proportional to airspeed. For example, consider two aircraft of vastly different wing loading ranges and assume the conversion factors x (g's/m/s) for aircraft #1 are known and we desire to scale those to aircraft #2. Then we know that

$$x_1 \sim \frac{V_1}{(W/S)_1} \text{ and } x_2 \sim \frac{V_2}{(W/S)_2} \tag{36}$$

where V and W/S represents the airspeed and the wing loading respectively of the vehicle of interest. Also, let λ_1 and λ_2 be factors that renders the above two proportions an equality. Then,

$$x_1 \equiv \lambda_1 \frac{V_1}{(W/S)_1} \text{ and } x_2 \equiv \lambda_2 \frac{V_2}{(W/S)_2} \tag{37}$$

with the implication that

$$x_2 = x_1 \left[\frac{\lambda_2}{\lambda_1}\right] \left[\frac{(W/S)_1}{(W/S)_2}\right] \left[\frac{V_2}{V_1}\right] \tag{38}$$

The key assumption underlying the similarity scaling technique is $\lambda_1 \approx \lambda_2$ and is based on the notion that conventional fixed-wing commercially-operated aircraft have similar flying and handling qualities. The lambda coefficients introduced above are largely dependent on aircraft stability and control parameters, which dictates the modal frequency and damping characteristics of aircraft longitudinal dynamic response to turbulence. The frequency and damping characteristics must lie in a relatively small range of values in order to achieve satisfactory handling qualities for conventional fixed-wing aircraft designs. Further details can be found in Reference [8] where the ranges of frequency and damping are expressed in terms of iso-contours of constant handling qualities based on pilot opinion.

Applying the basic ideas presented above, a final similarity scaling law can be written and a verification analysis conducted. The functional form of the similarity scaling law for the nine aircraft considered is given by:

$$x_n = x_0\big(V_0(h)\big) \times \left[\frac{E[(W/S)_0]}{(W/S)_n}\right] \times \left[\frac{V_n(h)}{V_0(h)}\right], n = 1 \ldots 9 \tag{39}$$

where:

$x_0\big(V_0(h)\big)$ = A Gaussian random variable for Class A systems as defined in Figure 8

$E[(W/S)_0]$ = Class A population mean statistic based on over nine hundred thousand flight operations

$\left[\frac{V_n(h)}{V_0(h)}\right]$ = Speed adjustment ratio based on OEM data collection process for the nine aircraft considered

$[(W/S)_n]$ = Wing loading range values for which OEM data was collected for the nth aircraft

In the above development, subscript zero refers to the data model associated with the population of Class A aircraft systems and W/S is defined as wing loading in lbs/ft^2. The units of x in all cases are g's/m/s. The index n identifies any one of the nine aircraft defined in Table 4.

Since x_0 is defined as a Gaussian random variable, then x_n is a Gaussian random variable with expected value $E[x_n]$ and standard deviation $\sigma(x_n)$ given by

$$E[x_n] = \mu_{x_0} \left[\frac{E[(W/S)_0]}{(W/S)_n}\right] \times \left[\frac{V_n(h)}{V_0(h)}\right] \tag{40}$$

$$\sigma(x_n) = \sigma_{x_0} \left[\frac{E[(W/S)_0]}{(W/S)_n}\right] \times \left[\frac{V_n(h)}{V_0(h)}\right] \tag{41}$$

where μ_{x_0} and σ_{x_0} are the mean and standard deviation for Class A systems as defined in Figure 8. Figure 10 through Figure 14 show comparisons of scaled results $E[x]$ to those calculated from OEM provided response data for two specific aircraft types. Both a Class B and Class C aircraft were selected to demonstrate typical results of the verification analysis.

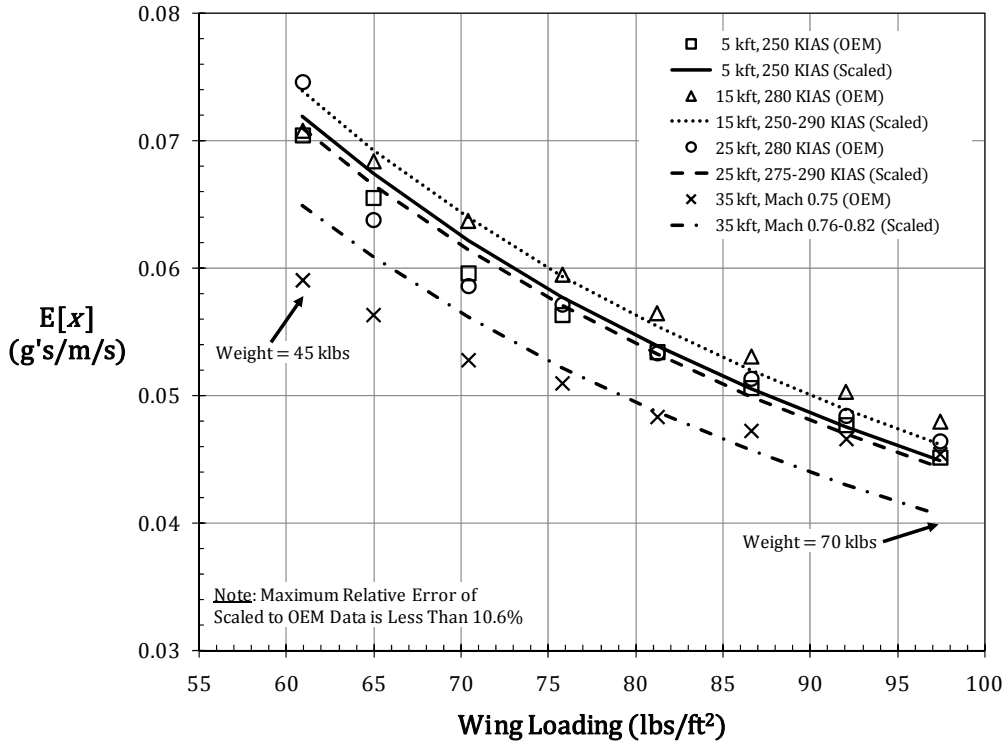

Figure 10: Comparison of Scaled and OEM Data for a Class B Aircraft at 5,000 ft; 15,000 ft; 25,000 ft; and 35,000 ft

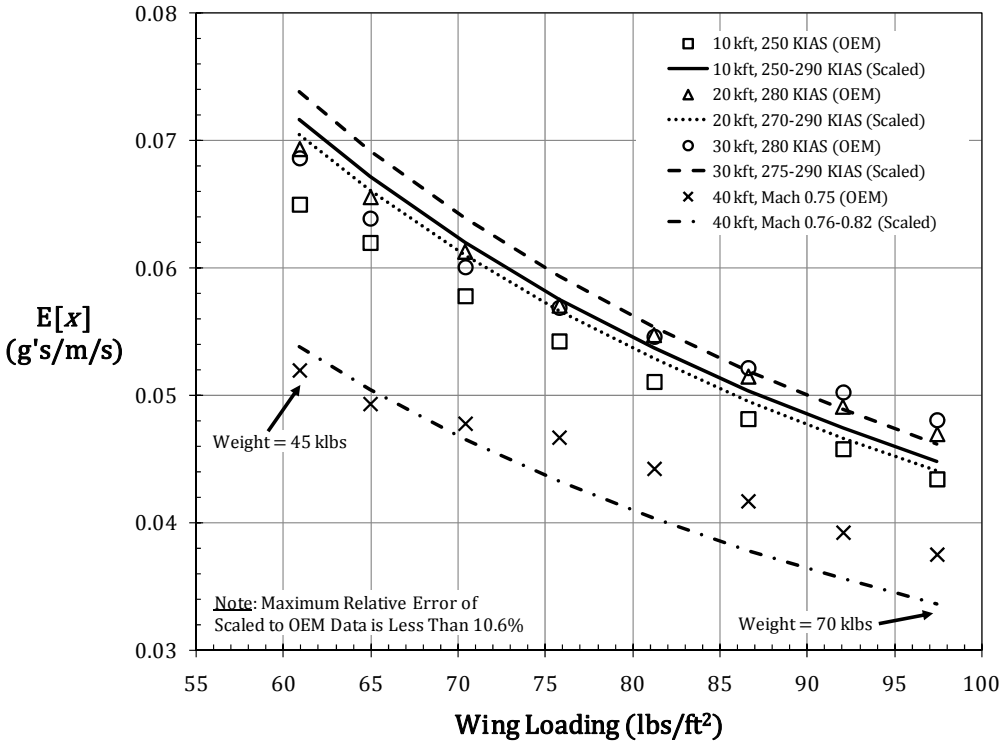

Figure 11: Comparison of Scaled and OEM Data for a Class B Aircraft at 10,000 ft; 20,000 ft; 30,000 ft; and 40,000 ft

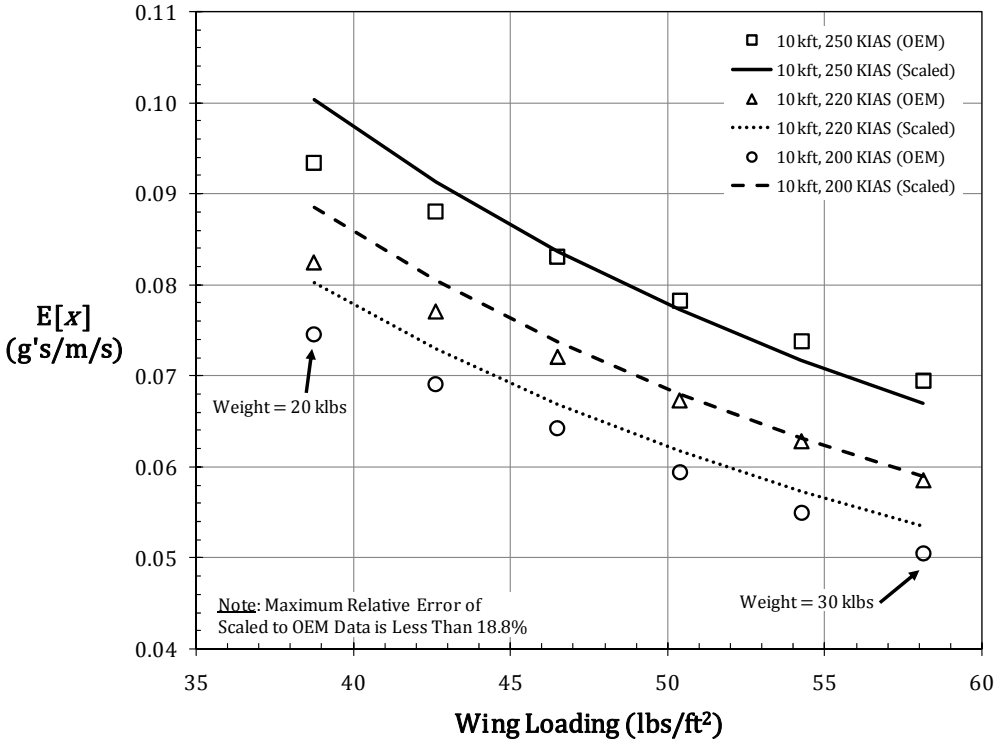

Figure 12: Comparison of Scaled and OEM Data for a Class C Aircraft at 10,000 ft

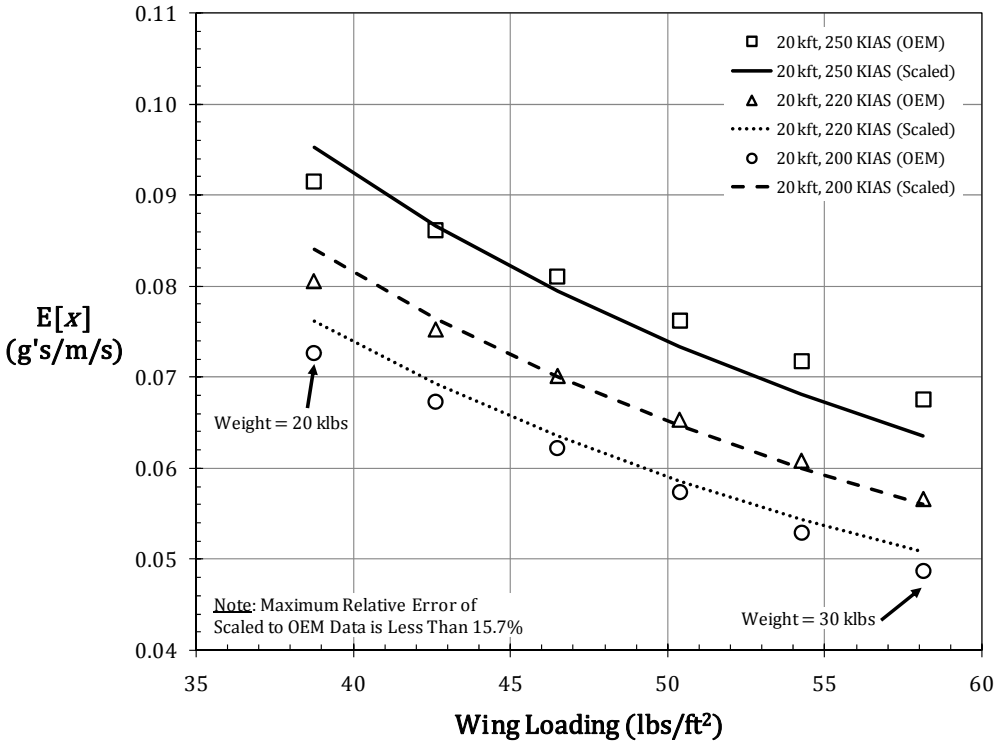

Figure 13: Comparison of Scaled and OEM Data for a Class C Aircraft at 20,000 ft

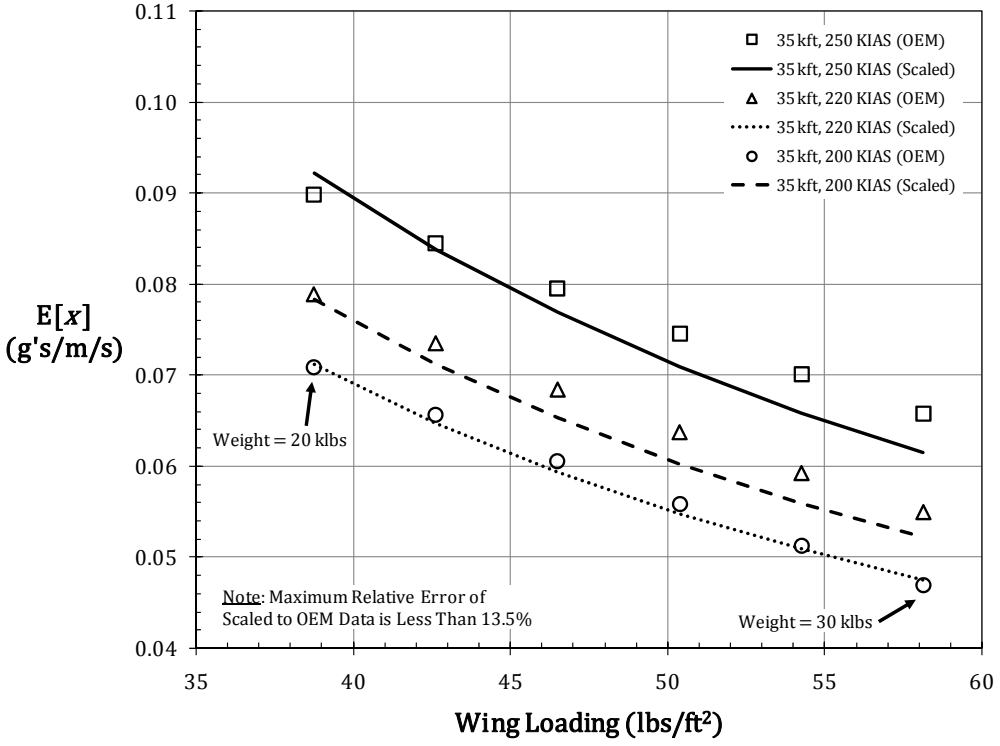

Figure 14: Comparison of Scaled and OEM Data for a Class C Aircraft at 35,000 ft

Equations (40) and (41) can be used to calculate the class based "one-size-fits-all" x-PDFs for Class B and C systems. In order to facilitate these calculations, it is necessary to quantify the class based wing-loading terms expressed in the denominator of Equations (40) and (41). These parameters were selected as the median value for the class being considered. The final results for the class based x-PDFs are shown in Figure 15 and Figure 16 and relevant data are summarized in Table 5 and Table 6.

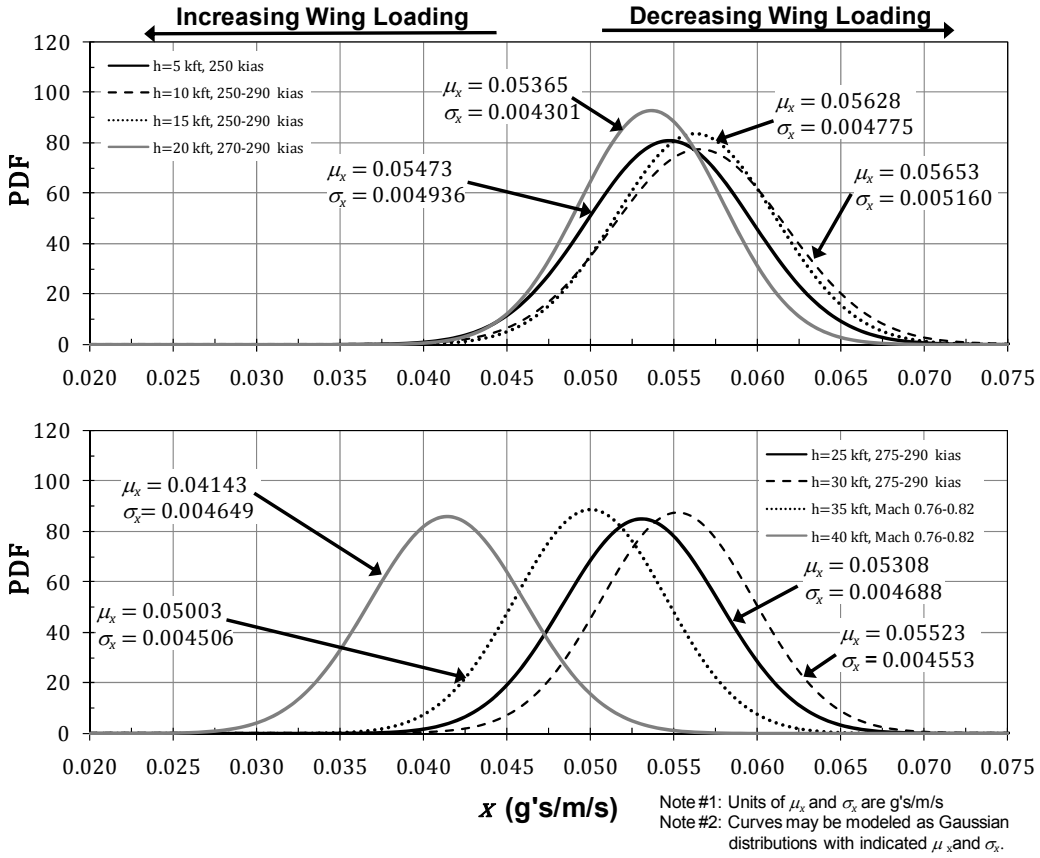

Figure 15: Class B Probability Density Functions for "One-Size-Fits-All" Algorithm Applicable for Aircraft Wing Loading between 60 and 100 lbs/ft^2

Table 5 lists the specific values for each flight condition present within the "one-size-fits-all" design for Class B aircraft systems.

Table 5: Class B Probability Density Functions for "One-Size-Fits-All" Algorithm Applicable for Aircraft Wing Loading between 60 and 100 lbs/ft^2

Flight Condition		PDF Conversion Factor	
Altitude (kft)	Airspeed (kias/Mach No.)	Mean, μ_x (g's/m/s)	Standard Deviation, σ_x (g's/m/s)
5	250	0.05473	0.004936
10	250-290	0.05653	0.005160
15	250-290	0.05628	0.004775
20	270-290	0.05365	0.004301
25	275-290	0.05308	0.004688
30	275-290	0.05523	0.004553
35	0.76-0.82	0.05003	0.004506
40	0.76-0.82	0.04143	0.004649

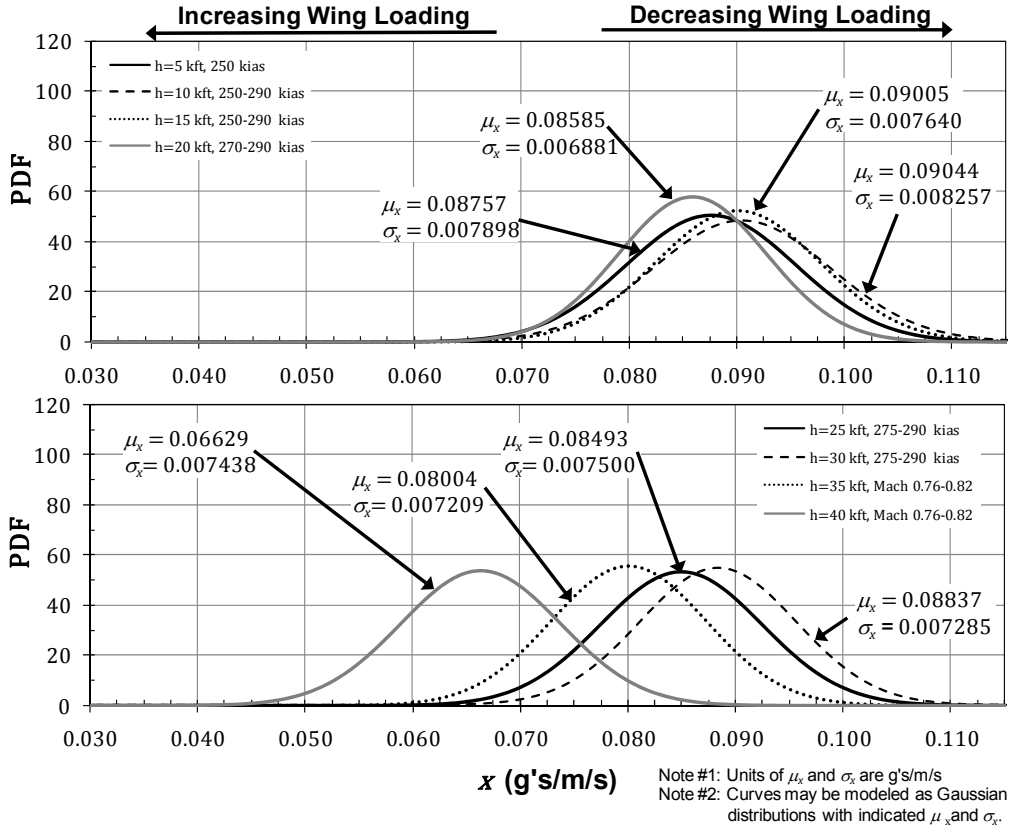

Figure 16: Class C Probability Density Functions for "One-Size-Fits-All" Algorithm Applicable for Aircraft Wing Loading between 30 and 70 lbs/ft^2

Table 6 lists the specific values for each flight condition present within the "one-size-fits-all" design for Class C aircraft systems.

Table 6: Class C Probability Density Functions for "One-Size-Fits-All" Algorithm Applicable for Aircraft Wing Loading between 30 and 70 lbs/ft^2

Flight Condition		PDF Conversion Factor	
Altitude (kft)	Airspeed (kias/Mach No.)	Mean, μ_x (g's/m/s)	Standard Deviation, σ_x (g's/m/s)
5	250	0.08757	0.007898
10	250-290	0.09044	0.008257
15	250-290	0.09005	0.007640
20	270-290	0.08585	0.006881
25	275-290	0.08493	0.007500
30	275-290	0.08837	0.007285
35	0.76-0.82	0.08004	0.007209
40	0.76-0.82	0.06629	0.007438

The curves shown in Figure 15 and Figure 16 and the data listed in Table 5 and Table 6 may be modeled as Gaussian distributions with means and standard deviations as indicated for each flight condition. These probability density functions are acceptable for typical airplanes with wing loading between 60 and 100 lbs/ft^2 and 30 and 70 lbs/ft^2 respectively throughout the entire flight regime. For airborne radar turbulence systems intended for installation on non-typical aircraft with configurations or wing loading outside this

range; the impact of configuration and wing loading must be considered when calculating the probability of missed detection and false positive turbulence indications.

8. Radar Spectrum Width PDFs Based on Published Data

In order to apply the methodology developed in the previous sections of this report, the radar probability density functions (y-random variable) and relevant statistics must be known. An applicant seeking certification approval for an E-Turb Radar system should provide the radar measurement statistics and probability density functions necessary to demonstrate compliance for the specific radar performance characteristics and configuration considered. Radar manufacturers typically employ simulation techniques for determining radar signal return time series from turbulent weather and radar signal processing for Doppler second moment estimation. However, manufacturers consider details regarding algorithms, range and cross range spatial filtering techniques, specific radar parameters, and resulting performance data as proprietary. Therefore, in order to perform calculations to demonstrate the methodology developed in the previous sections, with performance results, a public domain source of required data and spectrum width statistics was sought.

An available public data source for radar spectrum width statistics for modeling the y–probability density function can be found on page 138 (Fig. 6.6) of Doviak & Zrnić (Reference [9]). The FAA-ATDS working group has agreed that these data are representative of airborne radar Doppler second moment estimator performance, and is suitable for demonstrating the methodology developed in this report. The data found in Reference [9] are based on the fundamental assumption that the distribution of Doppler frequency of turbulent weather weighted by the antenna beam illumination and weather reflectivity is described by a Gaussian function. The performance data shown in Fig 6.6 of Reference [9] is based on autocovariance processing (pulse-pair) estimator of spectrum width for a single power weighted spectrum width measurement of narrow width relative to Nyquist frequency. The statistical data shown in Fig 6.6 of Reference [9] is in normalized form and can be rendered dimensional by choosing specific radar system parameters. The parameters selected, which are typical for airborne radars, are defined below:

c	= speed of light, $3\text{x}10^8$ m/s
f	= frequency, $9.3\text{x}10^9$ Hz
prf	= pulse repetition frequency (pulses/second), 3000 Hz
$\lambda = c/f$	= wavelength, 0.0323 m
$T_s = 1/prf$	= time between uniform samples, $3.333\text{x}10^{-4}$ s
$v_a = 1/(4T_s)$	= unambiguous velocity, 24.23 m/s
S/N	= single pulse signal-to-noise ratio, ≈ 15 dB

Dimensional data for the standard deviation of estimated spectrum width, plotted as a function of mean spectrum width estimate, is shown in Figure 17.

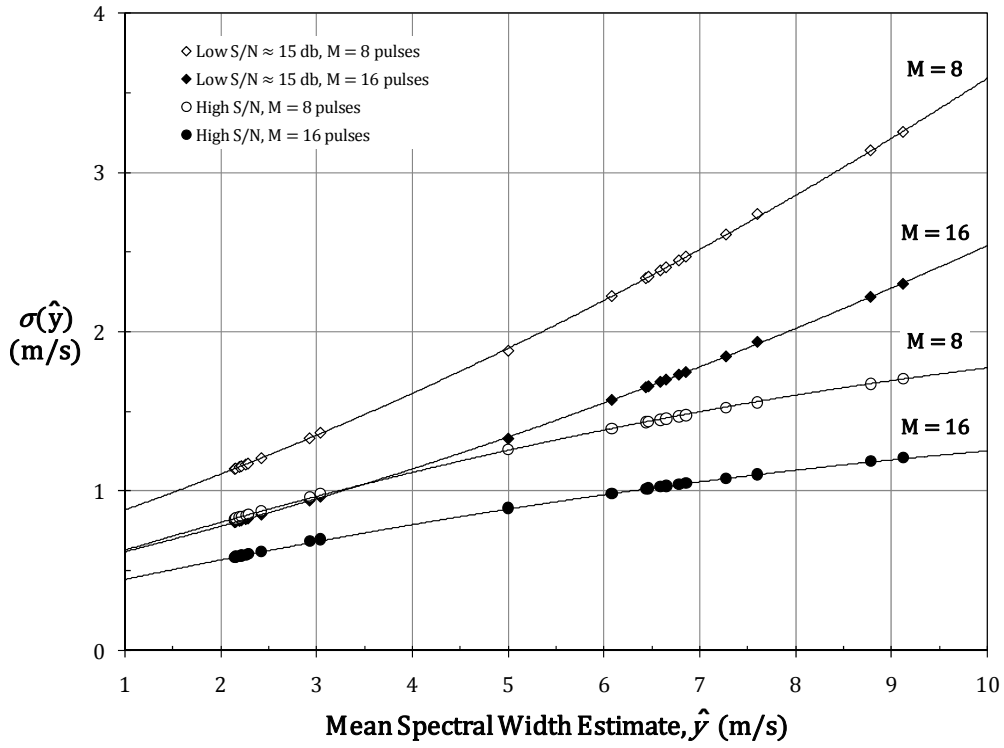

Figure 17: Standard Deviation of Autocovariance (Pulse Pair) Estimator vs. Mean Spectral Width

The data shown in Figure 17 are based on the radar parameters and assumptions stipulated above and M refers to the number of pulses processed by the estimator. The y–probability density function can now be written as:

$$f_y(y|y \geq 0) = \frac{C}{\sqrt{2\pi}\sigma(\hat{y})} exp\left[-\frac{1}{2}\left(\frac{y-\hat{y}}{\sigma(\hat{y})}\right)^2\right] \tag{42}$$

where:

$\sigma(\hat{y})$ = Standard Deviation of $\hat{y}$

$\hat{y}$ = Mean of y

C = Normalizing Constant, $\frac{1}{1-F_y(0)}$

9. Application of Defined Methodology with Results for Class A Aircraft Systems

The following text demonstrates the developed end-to-end methodology for calculating the must indicate and the must not indicate probabilities as defined in the previous sections of this report. Application of the "one-size-fits-all" model as well as a comparison to a "weight-strapped" implementation for the A320-200 and B777-200 aircraft is considered for a variety of flight conditions. Statistical performance results for representative E-Turb Radar system parameters are calculated, and results compared for the two systems implementations. Statistical performance results are presented in the form of a curve called the receiver operating characteristic. The terms of reference for the analysis are as follows:

- Two diverse aircraft types (A320-200 & B777-200) are selected.
- Extreme operating weights (light & heavy) are used for each aircraft type.

- For each aircraft type and weight, two different flight conditions (altitude and airspeed) are considered (low and slow, high and fast).
- Conversion factor x-values for weight-strapped implementation are based on hazard table data previously developed.
- For the "one-size-fits-all" implementation, the x-PDFs are defined in Figure 8 of Section 6.
- The same radar characteristics/parameters are used throughout the analysis. The specific radar parameters and y-PDFs are defined in Section 8. A 15 dB signal to noise ratio (S/N) is assumed, and M = 8 pulses selected for spectrum width estimator (pulse-pair) processing.

All of the calculations of probabilities are performed at an assumed 20 nautical mile radar range. At this assumed range, the pulse volume compensation factor (k) approaches a value of approximately 1 over a broad range of radar pulse lengths and antenna sizes (see Appendix I). Given the above terms of reference, specific numerical data needed for the calculation is shown in Table 7, where x^0 represents the hazard table value for a specific aircraft, weight, and airspeed configuration.

Table 7: Weight Strapped x^0 Values

A320-200			B777-200		
Weight (klbs)	Altitude Airspeed	x^0 (g's/m/s)	Weight (klbs)	Altitude Airspeed	x^0 (g's/m/s)
90	h = 5 kft V = 250 kias	0.0611	360	h = 5 kft V = 250 kias	0.0564
170*	h = 5 kft V = 250 kias	0.0386	640*	h = 5 kft V = 250 kias	0.0358
90	h = 35 kft M = 0.76	0.0564	360	h = 37 kft M = 0.82	0.0521
160*	h = 35 kft M = 0.76	0.0324	480*	h = 37 kft M = 0.82	0.0442

Data required to support the calculations for the "one-size-fits-all" model are provided in Figure 8 of Section 6 and Figure 17 of Section 8. These data, for the specific flight conditions selected, are shown in Table 8 below, including the radar mean spectrum width required to set the must indicate and must not indicate necessary conditions. The numerical data shown in Table 8 allow for complete specification of the x PDFs as defined in Figure 8 of Section 6 and y PDFs as defined by Equation (42). For the conditions stipulated above, these x and y PDFs enable direct calculation of the hazard metric z-PDF defined by Equation (6).

Table 8: Data Required for Calculating Must Indicate and Must Not Indicate Probabilities for the "One-Size-Fits-All" Model

Condition	Altitude Airspeed	μ_x (g's/m/s)	σ_x (g's/m/s)	$\hat{y}$ (m/s)	$\sigma_{\hat{y}}$ (m/s)
Must Not Indicate $\mu_z = 0.1$g	h = 5 kft V = 250 kias	0.04514	0.004071	2.215	1.159
	h = 35 kft M = 0.78 – 0.82	0.04126	0.003716	2.424	1.209
Must Indicate $\mu_z = 0.3$g	h = 5 kft V = 250 kias	0.04514	0.004071	6.646	2.403
	h = 35 kft M = 0.78 – 0.82	0.04126	0.003716	7.271	2.609

* Value represents the maximum weight for this aircraft type at this speed and altitude.

The probability of correct detection (must indicate) of turbulence conditions plotted as a function of a probability of nuisance detection (must not indicate) is shown in Figure 18 through Figure 21. The "one-size-fits-all" performance results shown in Figure 18 through Figure 21 were calculated using Equations (33) and (34) as was the weight strapped results for a range of positive z-threshold values. The results shown in the figures permit a direct comparison of "one-size-fits-all" and weight strapped system performance for most extreme operating weights at the indicated flight conditions.

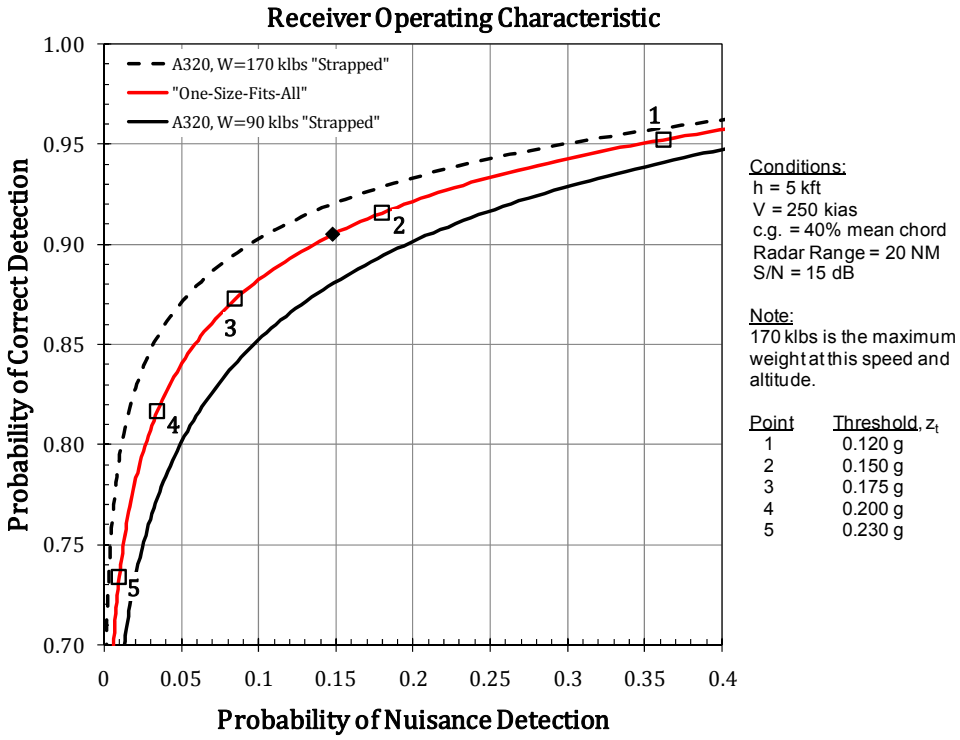

Figure 18: Comparison of "One-Size-Fits-All" Performance and A320-200 with Weight Strapped Results for Extreme Operating Weights at Indicated Flight Conditions (5,000 ft)

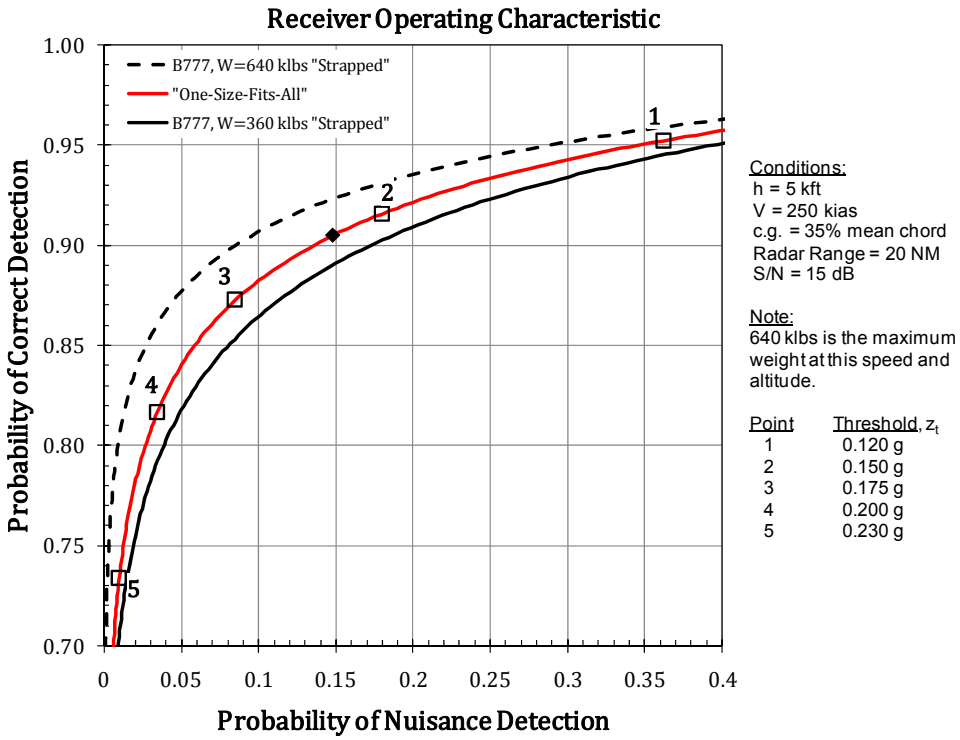

Figure 19: Comparison of "One-Size-Fits-All" Performance and B777-200 with Weight Strapped Results for Extreme Operating Weights at Indicated Flight Conditions (5,000 ft)

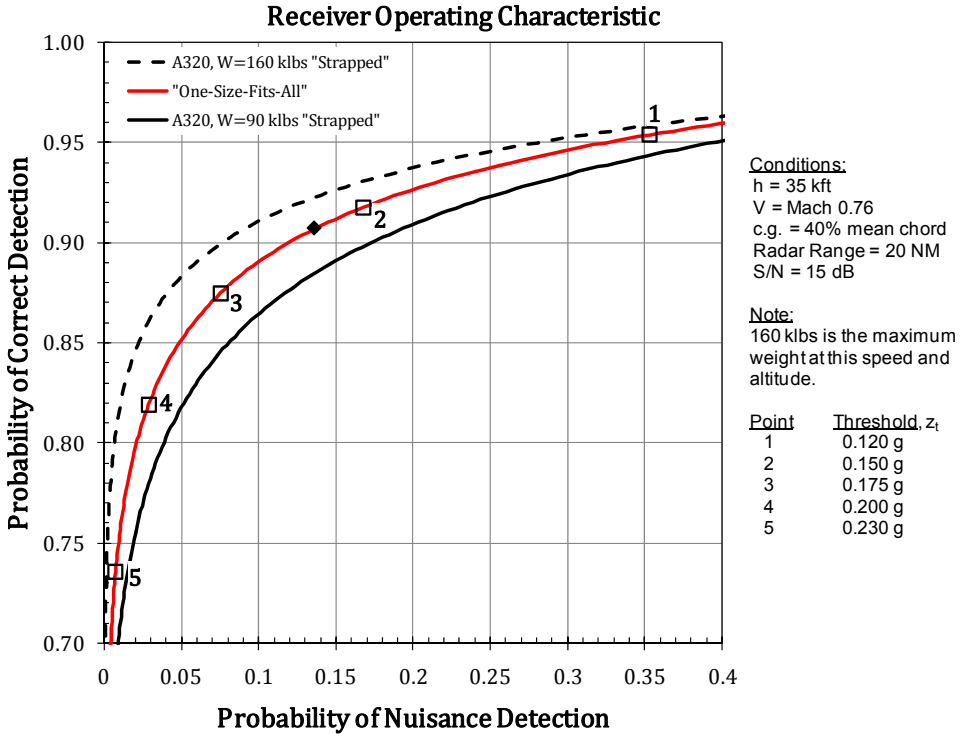

Figure 20: Comparison of "One-Size-Fits-All" Performance and A320-200 with Weight Strapped Results for Extreme Operating Weights at Indicated Flight Conditions (35,000 ft)

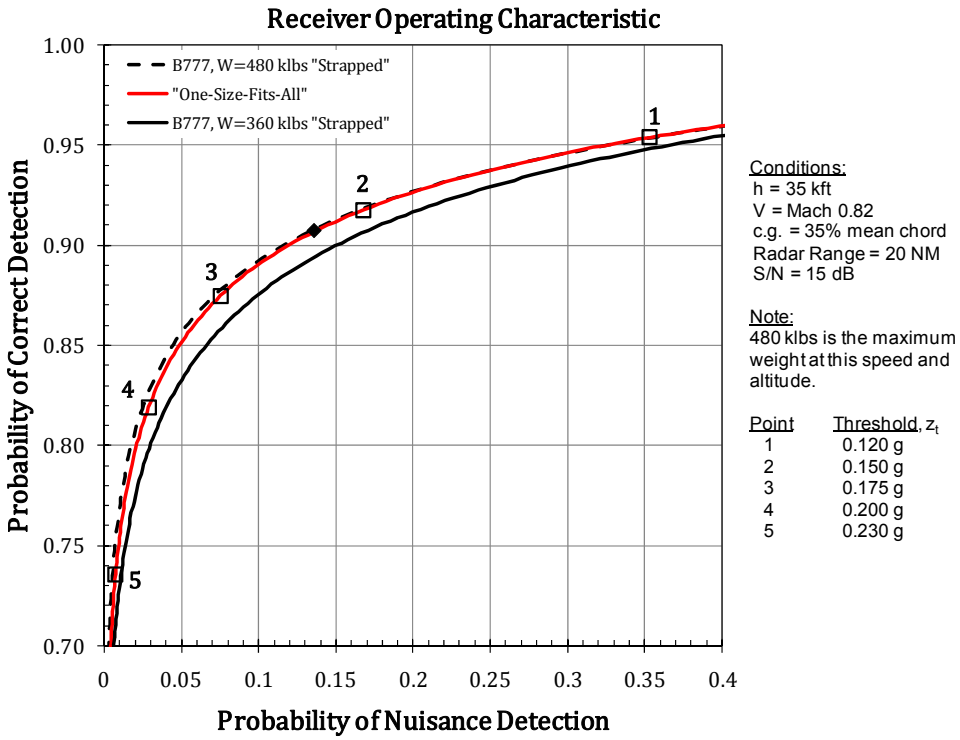

Figure 21: Comparison of "One-Size-Fits-All" Performance and B777-200 with Weight Strapped Results for Extreme Operating Weights at Indicated Flight Conditions (35,000 ft)

Note that the "one-size-fits-all" curves shown in the above figures are identical for the same specific flight condition considered and independent of aircraft type at that flight condition. This observation is consistent with the "one-size-fits-all" design philosophy, as long as the aircraft is in the class of large commercial transports with wing loading in the range of 80 – 135 lbs/ft^2 (Class A). The results shown in Figure 18 through Figure 21 clearly demonstrate robustness of the "one-size-fits-all" algorithm statistical design philosophy when compared to the more correct "weight strapped" implementation. For the cases considered in the analysis, there is no violation of the 85% correct turbulence indication versus 20% nuisance indication performance criteria, provided the proper system threshold is selected.

Also shown in Figure 18 through Figure 21 are results for five point set threshold values ranging from 0.12g to 0.23g. The point indicated by the diamond symbol in the above figures represents an "optimal" threshold, assuming the system cost of a missed correct turbulence indication is 2.5 times that of a nuisance indication. The optimal threshold calculation is based on the Bayes Criterion the details of which can be found in Reference [10], and assumes a prior probability of 0.5 that hypothesis H2 as defined in Figure 6 is true. The numerical value optimal threshold was found to be approximately 0.157 g for both flight conditions considered in the analysis, thus indicating low sensitivity for the "one-size-fits-all" implementation.

10. Summary and Conclusions

The objective of the research developed and presented in this document was to statistically assess turbulence hazard detection performance employing airborne pulse Doppler radar systems. The FAA certification methodology for forward-looking airborne turbulence radars will require estimating the probabilities of missed and false hazard indications under operational conditions. Analytical approaches must be used due to the near impossibility of obtaining sufficient statistics experimentally. This report describes an end-to-end analytical technique for estimating these probabilities for E-Turb Radar systems

under noise-limited conditions, for a variety of aircraft types, as defined in FAA TSO-C134. This technique provides for one means, but not the only means, by which an applicant can demonstrate compliance to the FAA directed ATDS Working Group performance requirements. Turbulence hazard algorithms were developed that derived predictive estimates of aircraft hazards from basic radar observables. These algorithms were designed to prevent false turbulence indications while accurately predicting areas of elevated turbulence risks to aircraft, passengers, and crew; and were successfully flight tested on a NASA B757-200 and a Delta Air Lines' B737-800. Application of this methodology for calculating the probability of missed and false hazard indications, taking into account the effect of the various algorithms used, is demonstrated for representative transport aircraft and radar performance characteristics.

11. References

[1] Prince, J. B., Buck, B. K., Robinson, P. A., and Ryan, T., "In-Service Evaluation of the Turbulence Auto-PIREP System and Enhanced Turbulence Radar Technologies," NASA Contractor Report Series, NASA/CR-2007-214887, Hampton, Virginia, July 2007.

[2] U.S. Department of Transportation. Federal Aviation Administration. Aircraft Certification Service, Technical Standard Order. *TSO-C134: Airborne Doppler Weather Radar With Forward-Looking Turbulence Detection Capability*, Washington D.C., Effective Date: *Pending*.

[3] Hoblit, Frederic M. Gust Loads on Aircraft: Concepts and Applications. American Institute of Aeronautics and Astronautics, Inc., Washington D.C., 1988.

[4] "In-flight Aviation Weather Advisories", NOAA National Weather Service Directive ND229107, May 22, 1991.

[5] Hamilton, D. and Proctor, F., "Airborne Turbulence Detection System Certification Tool Set," AIAA-2006-75, 44th AIAA Aerospace Sciences Meeting and Exhibit, Reno, Nevada, Jan. 9-12, 2006.

[6] Gnedkenko, Boris V. The Theory of Probability, 4th Edition. Chelsea Publishing Company, New York, New York, 1967.

[7] "Airplane Simulation Qualification," AC120-40B, Department of Transportation, Federal Aviation Administration, July 29, 1991.

[8] O'Hara, F. "Handling Criteria." Journal of the Royal Aeronautical Society, Vol. 71, No. 676, pp. 271-291, 1967.

[9] Doviak, Richard J. and Zrinć, Dušan S. Doppler Radar and Weather Observations, 2nd Edition. Dover Publications, Inc., Mineola, New York, 2006.

[10] Helstrom, Carl W. Statistical Theory of Signal Detection. Pergamon Press, New York, New York, 1960.

Appendix I

Calculation of Pulse Volume Compensation Factor

The following defines the symbology used within this appendix:

c = Speed of light, 3×10^8 m/s

$E(k)$ = Turbulence energy spectra as a function of k

k = Turbulence wave number (rad/m)

L = Turbulence scale length (m)

R = σ_r/σ_θ, characteristic range (m)

r = Radar range (m)

μ = $a'L/\sigma_r$ (non-dimensional), where $a' = 1.339$

θ_1 = One-way antenna beam width between half-power points (rad)

σ = RMS turbulence intensity of the one-dimensional von Kármán energy spectra (m/s)

σ_θ = Transverse 2nd central moment of a two-way Gaussian beam illumination function[1] (rad)

σ_r = Radial 2nd central moment of a two-way Gaussian beam illumination function[2] (m)

σ_v = Doppler velocity spectrum width (m/s)

τ = Radar pulse width (s)

The radar pulse volume filtering phenomenon was introduced and discussed in Section 3 of the main body of the report. Specific techniques for compensating these effects are presented in this appendix. Specifically, a theoretical relationship between radar spectrum width (2nd moment measurements) and turbulent velocity point variance must be defined. In order to develop this relationship, the following assumptions are made:

1. The turbulence wind field is characterized by the universe of realizations based on von Kármán energy spectra. The turbulent wind field is assumed homogeneous and isotropic.
2. It is assumed that the reflectivity within the radar resolution volume is uniform, with adequate signal-to-noise for reliable Doppler processing.
3. A Gaussian two-way beam illumination function is assumed with one parameter transverse to and the other along the radar beam.
4. The radar observable is assumed to be a spectrum width product with all spectrum width broadening artifacts removed.
5. A 9.3 GHz X-band radar is assumed with matching receiver bandwidth for a transmitted rectangular pulse.
6. A two-way circular symmetric antenna pattern is assumed with no antenna losses and a diameter of 28 inches.

[1] Equation 5.67, p89. Doviak, Richard J. and Zrinć, Dušan S. Doppler Radar and Weather Observations, Academic Press, San Diego, California, 1984.

[2] Equation 5.68, p89. Doviak, Richard J. and Zrinć, Dušan S. Doppler Radar and Weather Observations, Academic Press, San Diego, California, 1984. Assumes a rectangular transmitted pulse and a matched Gaussian receiver frequency response.

For the conditions stipulated above it has been shown[3], with additional prior elaboration by others[4], that the connection between radar Doppler spectrum width and turbulence energy spectra is given by an indefinite integral:

$$\langle\sigma_v^2(r)\rangle = \frac{1}{4\pi}\iiint \frac{E(k)}{k^2}\left(1-\frac{k_z^2}{k^2}\right)\left[1-\exp\left(-a^2\left(k_x^2+k_y^2\right)-b^2k_z^2\right)\right]dk_x\,dk_y dk_z \tag{I-1}$$

The above equation expresses the ensemble average of the radar spectrum width at a range r, in terms of turbulent energy spectra $E(k)$ and radar system parameters. The subscripted k's indicate the components of the turbulent spatial wave numbers in units of rad/m and k (not to be confused with the k defined in Section 3) is the magnitude of the wave number vector. For a specific radar and antenna design the parameters a and b are constants and are defined as:

$$a = r\sigma_\theta = \frac{r\theta_1}{(8\ln 4)^{0.5}} \tag{I-2}$$

$$b = \sigma_r = 0.35\left(\frac{c\tau}{2}\right) \tag{I-3}$$

If a specific form of turbulent energy spectrum is known, and a particular radar configuration assumed, then estimates of radar spectrum width can be made by calculating Equation (I-1). In order to facilitate calculation of Equation (I-1), it is convenient to introduce polar spherical coordinates in k-wave number space, where the coordinate system is rotated such that the z-axis is along the radar radial line of sight. For this coordinate system alignment, direct integration over the polar spherical angles can be carried out resulting in the following equations.

$$\langle\sigma_v^2(r)\rangle = \frac{2}{3}\int_{k_0}^{\infty} E(k)\left[1-e^{-a^2k^2}M\left(\frac{1}{2},\frac{5}{2},(a^2-b^2)k^2\right)\right]dk \text{ for } a \geq b \tag{I-4}$$

$$\langle\sigma_v^2(r)\rangle = \frac{2}{3}\int_{k_0}^{\infty} E(k)\left[1-e^{-b^2k^2}M\left(2,\frac{5}{2},(b^2-a^2)k^2\right)\right]dk \text{ for } b > a \tag{I-5}$$

Where $k_0 = \frac{2\pi}{\lambda_0}$ and $\lambda_0$is equal to the turbulence "outer scale" wavelength.

In the above equations, $M(\alpha,\gamma,\xi)$ is the confluent hypergeometric function which is formally defined as:

$$M(\alpha,\gamma,\xi) = \frac{\Gamma(\gamma)}{\Gamma(\alpha)}\sum_{n=0}^{n=\infty}\frac{\Gamma(n+\alpha)}{\Gamma(n+\gamma)}\frac{\xi^n}{n!} \tag{I-6}$$

The above sum is a convergent series for all positive values of the three arguments.

A specific form of turbulent energy spectra, $E(k)$, is needed in order to evaluate Equations (I-4) and (I-5). It is assumed that $E(k)$ is given by the von Kármán spectra, which are functionally defined as:

$$E(k) = \frac{55}{9}\frac{\sigma^2 L}{\pi}\frac{(a'Lk)^4}{[1+(a'Lk)^2]^{17/6}} \tag{I-7}$$

Where σ is the RMS turbulence intensity (m/s) and L is the turbulence scale length (m).

[3] Chapter 10. Doviak, Richard J. and Zrinć, Dušan S. Doppler Radar and Weather Observations, Academic Press, San Diego, California, 1984.

[4] Frisch, A. S. and Clifford, S. F. "A Study of Convection Capped by a Stable Layer Using Doppler Radar and Acoustic Echo Sounders," Journal of Atmospheric Sciences, Volume 31, No. 6, 1974.

Substitution of Equation (I-7) into Equations (I-4) and (I-5) and assuming $k_0 = 0$ yields:

$$\frac{\langle \sigma_v^2(r) \rangle}{\sigma^2} = 1 - \frac{55}{27} \cdot \frac{1}{\pi a'} \cdot \mu^5 \int_0^\infty \frac{x^{3/2} e^{-x}}{[1+\mu^2 x]^{17/6}} \cdot M\left[2, \frac{5}{2}, \left(1 - \frac{r^2}{R^2}\right) x\right] dx \qquad \text{(I-8)}$$

for $0 \leq r < R$

$$\frac{\langle \sigma_v^2(r) \rangle}{\sigma^2} = 1 - \frac{55}{27} \cdot \frac{1}{\pi a'} \cdot \mu^5 \int_0^\infty \frac{x^{3/2} e^{-(r/R)^2 x}}{[1+\mu^2 x]^{17/6}} \cdot M\left[\frac{1}{2}, \frac{5}{2}, \left(\frac{r^2}{R^2} - 1\right) x\right] dx \qquad \text{(I-9)}$$

for $R \leq r$

Where the independent variable of integration x (not to be confused with x defined in Section 3 of the main body of this report) is defined as $x = \sigma_r^2 k^2$.

All other parameters indicated in Equations (I-8) and (I-9) are defined in the nomenclature section of this appendix. The authors have not found Equations (I-8) and (I-9) in the open literature, although they were developed using methods outlined in Footnote #1 of Appendix I, and the authors believe these equations offer distinct numerical computational advantages. The specific form of the energy spectra employed in the above development is known to contain the Kolmogorov inertial subrange, in which energy cascades from large eddies to smaller eddies, with eventual dissipation by viscous forces. However, the above derivation is not limited to this assumption, which is typical practice within the industry, since larger wavelengths can have significant impact on turbulence response of aircraft depending on speed and other design factors.

Figure I - 1 shows the pulse volume compensation factor calculation results using Equations (I-8) and (I-9) plotted as a function of radar range for several selected radar pulse lengths. The specific parameters selected for the calculation are: –3 dB antenna beam width of 3.8 deg, turbulence length scale of 500 m, turbulence outer scale wave number of zero, and four radar pulse lengths were selected.

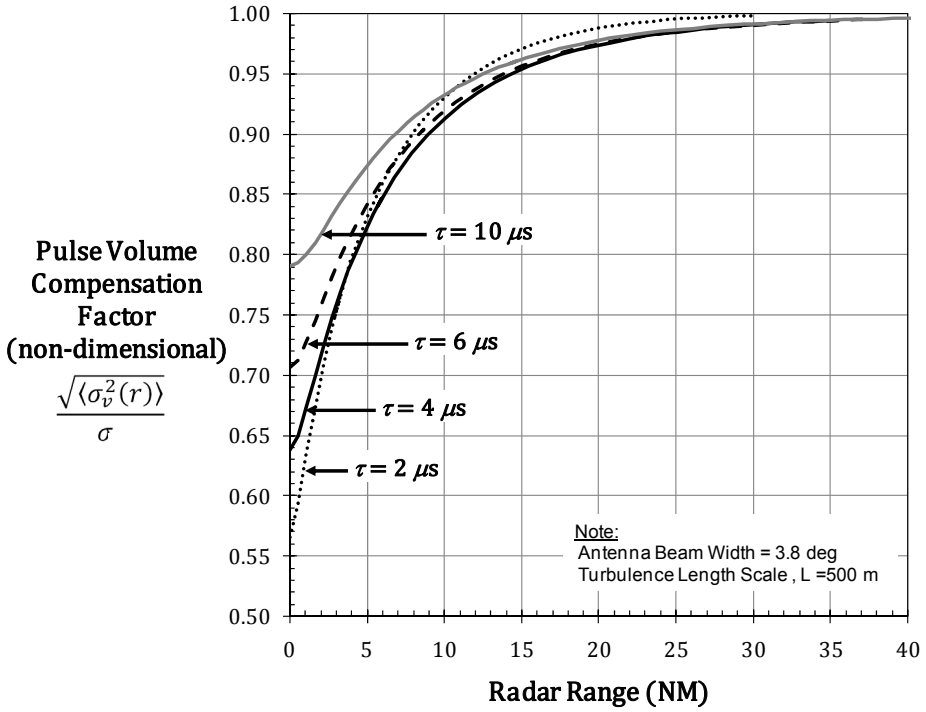

Figure I - 1: Pulse Volume Compensation Factor versus Radar Range

Note that the pulse volume compensation factor k as defined in Section 3 of the main body of this report is given by:

$$k(r, \tau, \ldots) = \frac{1}{\frac{\sqrt{\langle \sigma_v^2(r) \rangle}}{\sigma}} \tag{I-10}$$

For radar ranges greater than 20-25 nautical miles k takes on values of approximately one. However, in the radar near field of view, where the resolution volume of the radar is of smaller spatial dimension, $k > 1$.

Appendix II

Inclusion of Radar Pulse Volume Compensation Factor in the Governing Probability Equations

If an applicant seeking certification approval elects to include radar pulse volume compensation for their system implementation, then the governing probability equations presented in the body of this report must be modified. The necessary modifications can be accomplished by employing probability density function transformation techniques found in Reference [6]. For example:

> If ζ is a random variable and $\lambda = a\zeta + b$ then $f_\lambda(\lambda) = \frac{1}{a} f_\zeta\left(\frac{\lambda - b}{a}\right)$ provided the equation $\lambda = a\zeta + b$ has a single solution of $\zeta = \frac{\lambda - b}{a}$ for every λ where a and b are constants.

Consider the "one-size-fits-all" model first. If the uncompensated process $z = xy$ has a z-PDF given by Equation (6):

$$p_z(z|z \geq 0) = N \int_0^\infty \frac{f_y(y) f_x(z/y)}{y} dy \tag{II-1}$$

then using the above transformation, the PDF for the compensated process $z = kxy$ is given by:

$$p_z(z|z \geq 0) = \frac{N}{k} \int_0^\infty \frac{f_y(y) f_x(z/(ky))}{y} dy \tag{II-2}$$

The compensation factor k is a constant at a specified radar range and choice of radar system parameters. Using Equation (II-2) the mean and variance of z can be directly calculated and are given by the following:

$$\mu_z = \int_0^\infty z p_z(z) dz = Nk\mu_x\mu_y \tag{II-3}$$

$$\sigma_z^2 = \int_0^\infty z^2 p_z(z) dz - \mu_z^2 = (Nk)^2 \left[\left(\sigma_x\sigma_y\right)^2 + \left(\mu_x\sigma_y\right)^2 + \left(\mu_y\sigma_x\right)^2\right] \tag{II-4}$$

For the pulse volume compensated "weight strapped" case, the system process is defined as $z = kx^0 y$ where x^0 is the hazard table value for a specific airplane, weight, and flight condition. The uncompensated ($k = 1$) z-PDF as defined by Equation (29) is:

$$p_z(z|z \geq 0) = \frac{N}{x^0} f_y\left(\frac{z}{x^0}\right) \text{ where } N = \frac{1}{1 - F_z(0)} \tag{II-5}$$

Using the transformation technique outlined above, the compensated z-PDF is given by:

$$p_z(z|z \geq 0) = \frac{N}{kx^0} f_y\left(\frac{z}{kx^0}\right) \tag{II-6}$$

where the mean and variance are given by :

$$\mu_z = \int_0^\infty z p_z(z) dz = Nkx^0\mu_y \tag{II-7}$$

$$\sigma_z^2 = \int_0^\infty z^2 p_z(z) dz - \mu_z^2 = \left(Nkx^0\sigma_y\right)^2 \tag{II-8}$$

REPORT DOCUMENTATION PAGE

Form Approved
OMB No. 0704-0188

1. REPORT DATE *(DD-MM-YYYY)*	2. REPORT TYPE	3. DATES COVERED *(From - To)*
01-06-2009	Contractor Report	October 2007 - May 2009

4. TITLE AND SUBTITLE
A Methodology for Determining Statistical Performance Compliance for Airborne Doppler Radar with Forward-Looking Turbulence Detection Capability

5a. CONTRACT NUMBER
NNL06AA03B

5b. GRANT NUMBER

5c. PROGRAM ELEMENT NUMBER

6. AUTHOR(S)
Bowles, Roland L.; and Buck, Bill K.

5d. PROJECT NUMBER

5e. TASK NUMBER
NNL08AC16T and NNL07AE19T

5f. WORK UNIT NUMBER

7. PERFORMING ORGANIZATION NAME(S) AND ADDRESS(ES)
NASA Langley Research Center
Hampton, VA 23681-2199

8. PERFORMING ORGANIZATION REPORT NUMBER
ATR-2009-12038

9. SPONSORING/MONITORING AGENCY NAME(S) AND ADDRESS(ES)
National Aeronautics and Space Administration
Washington, DC 20546-0001

10. SPONSORING/MONITOR'S ACRONYM(S)
NASA

11. SPONSORING/MONITORING REPORT NUMBER
NASA/CR-2009-215769

12. DISTRIBUTION/AVAILABILITY STATEMENT
Unclassified - Unlimited
Subject Category 03
Availability: NASA CASI (443) 757-5802

13. SUPPLEMENTARY NOTES
This report was prepared by AeroTech Research under subcontract to ARINC Inc., Annapolis, MD, NASA contract NNL06AA03B, Task Orders NNL08AC16T and NNL07AE19T. NASA Langley Technical Monitor: James F. Watson

14. ABSTRACT

The objective of the research developed and presented in this document was to statistically assess turbulence hazard detection performance employing airborne pulse Doppler radar systems. The FAA certification methodology for forward-looking airborne turbulence radars will require estimating the probabilities of missed and false hazard indications under operational conditions. Analytical approaches must be used due to the near impossibility of obtaining sufficient statistics experimentally. This report describes an end-to-end analytical technique for estimating these probabilities for E-Turb Radar systems under noise-limited conditions, for a variety of aircraft types as defined in FAA TSO-C134. This technique provides for one means, but not the only means, by which an applicant can demonstrate compliance to the FAA directed ATDS Working Group performance requirements. Turbulence hazard algorithms were developed that derived predictive estimates of aircraft hazards from basic radar observables. Application of this defined methodology for calculating the probability of missed and false hazard indications taking into account the effect of the various algorithms used, is demonstrated for representative transport aircraft and radar performance characteristics.

15. SUBJECT TERMS
Aviation Safety, Turbulence, Turbulence Detection, Turbulence Encounters, Turbulence Reporting, Doppler Radar, Enhanced Airborne Weather Radar, Enhanced Turbulence (E-Turb), Airborne Remote Sensing, Detection Probability, Turbulence Hazard Metric, Weather, Safety, TSO-C134.

16. SECURITY CLASSIFICATION OF:			17. LIMITATION OF ABSTRACT	18. NUMBER OF PAGES	19b. NAME OF RESPONSIBLE PERSON
a. REPORT	b. ABSTRACT	c. THIS PAGE			STI Help Desk (email: help@sti.nasa.gov)
					19b. TELEPHONE NUMBER *(Include area code)*
U	U	U	UU	48	(443) 757-5802